Space-Time Domain Decomposition Methods for Diffusion Problems in Mixed Formulations

Thi Thao Phuong Hoang, Jérôme Jaffré, Caroline Japhet, Michel Kern, Jean Roberts

Space-Time Domain Decomposition Methods for Diffusion Problems in Mixed Formulations

Thi Thao Phuong Hoang, Jérôme Jaffré , Caroline Japhet ,
Michel Kern , Jean E. Roberts

ISSN 0249-6399   ISRN INRIA/RR--8271--FR+ENG

RESEARCH REPORT
N° 8271
March 2013
Project-Teams POMDAPI

Space-Time Domain Decomposition Methods for Diffusion Problems in Mixed Formulations

Thi Thao Phuong Hoang[*†], Jérôme Jaffré [*], Caroline Japhet [*‡], Michel Kern [*], Jean E. Roberts [*]

Project-Teams POMDAPI

Research Report n° 8271 — March 2013 — 33 pages

Abstract: This paper is concerned with global-in-time, nonoverlapping domain decomposition methods for the mixed formulation of the diffusion problem. Two approaches are considered: one uses the time-dependent Steklov-Poincaré operator and the other uses Optimized Schwarz Waveform Relaxation (OSWR) based on Robin transmission conditions. For each method, a mixed formulation of an interface problem on the space-time interfaces between subdomains is derived, and different time grids are employed to adapt to different time scales in the subdomains. Demonstrations of the well-posedness of the subdomain problems involved in each method and a convergence proof of the OSWR algorithm are given for the mixed formulation. Numerical results for 2D problems with strong heterogeneities are presented to illustrate the performance of the two methods.

Key-words: mixed formulations, space-time domain decomposition, diffusion problem, time-dependent Steklov-Poincaré operator, optimized Schwarz waveform relaxation, nonconforming time grids

This work was partially supported by the GNR MoMaS (PACEN/CNRS, ANDRA, BRGM, CEA, EDF, IRSN)

[*] INRIA Paris-Rocquencourt, project-team Pomdapi, 78153 Le Chesnay Cedex, France
Emails: Phuong.Hoang_Thi_Thao@inria.fr, Jerome.Jaffre@inria.fr, Caroline.Japhet@inria.fr, Michel.Kern@inria.fr, Jean.Roberts@inria.fr

[†] Partially supported by ANDRA, the French agency of nuclear waste management

[‡] Université Paris 13, UMR 7539, LAGA, 99 Avenue J-B Clément, 93430 Villetaneuse, France
Email: japhet@math.univ-paris13.fr

RESEARCH CENTRE
PARIS – ROCQUENCOURT

Domaine de Voluceau, - Rocquencourt
B.P. 105 - 78153 Le Chesnay Cedex

Méthode de Décomposition de Domaine Espace-Temps pour les Problèmes de Diffusion en Formulation Mixte

Résumé : Ce papier traite de méthodes de décomposition de domaine sans recouvrement, globales en temps, appliquées à un problème de diffusion en formulation mixte. Deux approches sont considérées: l'une basée sur l'opérateur de Steklov-Poincaré, et l'autre basée sur une méthode de relaxation d'onde optimisée (OSWR), utilisant des conditions de transmission de type Robin. Pour chaque méthode, un problème d'interface est écrit sous forme mixte, les inconnues étant sur les interfaces espace-temps entre les sous-domaines, et différentes grilles en temps sont utilisées, adaptées aux différentes échelles temporelles dans les sous-domaines. Des démonstrations à la fois du caractère bien posé des problèmes locaux dans les sous-domaines (intervenant dans chaque méthode) et de la convergence de l'algorithm OSWR sont données en formulation mixte. Des résultats numériques pour des problèmes 2D avec de fortes hétérogénéités sont présentés pour illustrer les performances des deux méthodes.

Mots-clés : formulation mixte, décomposition de domaine espace-temps, problème de diffusion, opérateur de Steklov-Poincaré dépendant du temps, méthode de relaxation d'onde optimisée, maillages non-conformes en temps

1. Introduction. In many simulations of time-dependent physical phenomena, the domain of calculation is actually a union of several subdomains with different physical properties and in which the time scales may be very different. In particular, this is the case for the simulation of contaminant transport around a nuclear waste repository, where the time scales vary over several orders of magnitude due to changes in the hydrogeological properties of the various geological layers involved in the simulation. Consequently, it is inefficient to use a single time step throughout the entire domain. The aim of this article is to investigate, in the context of mixed finite elements [5, 30], two global-in-time domain decomposition methods well-suited to nonmatching time grids. Advantages of mixed methods include their mass conservation property and a natural way to handle heterogeneous and anisotropic diffusion tensors.

The first method is a global-in-time substructuring method which uses a Steklov-Poincaré type operator. For stationary problems, this kind of method (see [29, 34, 28]) is known to be efficient for problems with strong heterogeneity. It uses the so-called Balancing Domain Decomposition (BDD) preconditioner introduced and analyzed in [24, 25], and in [6] for mixed finite elements. In brief, the method "involves at each iteration the solution of a local problem with Dirichlet data, a local problem with Neumann data and a "coarse grid" problem to propagate information globally and to insure the consistency of the Neumann problems" [6].

The second method uses the Optimized Schwarz Waveform Relaxation (OSWR) approach. The OSWR algorithm is an iterative method that computes in the subdomains over the whole time interval, exchanging space-time boundary data through more general (Robin or Ventcel) transmission operators in which coefficients can be optimized to improve convergence rates. Introduced for parabolic and hyperbolic problems in [9], it was extended to advection-reaction-diffusion problems with constant coefficients in [26]. The optimization of the Robin (or Ventcel) parameters was analyzed in [10, 1] and extended to discontinuous coefficients in [11, 2]. Extensions to heterogeneous problems and non-matching time grids were introduced in [11, 3]. More precisely, in [3, 15], discontinuous Galerkin (DG) for the time discretization of the OSWR was introduced to handle non-conforming time grids, in one dimension with discontinuous coefficients. This approach was extended to the bidimensional case in [17, 18]. One of the advantages of the DG method in time is that a rigorous analysis can be carried out for any degree of accuracy and local time-stepping, with different time steps in different subdomains (see [17, 18]). A suitable time projection between subdomains was obtained by an optimal projection algorithm without any additional grid, as in [13]. These papers use Lagrange finite elements. An extension to vertex-centered finite volume schemes and nonlinear problems is given in [14]. The classical Schwarz algorithm for stationary problems with mixed finite elements was analyzed in [7].

In this work, we extend the first method to the case of unsteady problems and construct the time-dependent Steklov-Poincaré operator. For parabolic problems, we need only the Neumann-Neumann preconditioner [22] as there are no difficulties con-

*INRIA Paris-Rocquencourt, 78153 Le Chesnay Cedex, France (Phuong.Hoang_Thi_Thao@inria.fr, Jerome.Jaffre@inria.fr, Michel.Kern@inria.fr, Jean.Roberts@inria.fr)

‡Université Paris 13, UMR 7539, LAGA, 99 Avenue J-B Clément, 93430 Villetaneuse, France (japhet@math.univ-paris13.fr).

§Partially supported by ANDRA, the French agency of nuclear waste management

*Partially supported by GNR MoMaS.

cerning consistency for time-dependent Neumann problems. Of course one could make use of the idea of the "coarse grid" to ensure a convergence rate independent of the number of subdomains. However, we haven't developed this idea here. The convergence of a Jacobi iteration for the primal formulation is independently introduced and analyzed in [21].

For the second method, an extension of the OSWR method with Robin transmission conditions to the mixed formulation is studied and a proof of convergence is given. For each method a mixed formulation of an interface problem on the space-time interfaces between subdomains is derived. The well-posedness of the subdomain problems involved in the first approach is addressed in [23, 4], through a Galerkin method and suitable a priori estimates. In this paper we present a more detailed version of the proof for Dirichlet and extend these results to to prove the well-posedness of the Robin subdomain problems involved in the OSWR approach. In [31, 32] demonstrations using semigroups are given for nonlinear evolution problems. For strongly heterogeneous problems, it is natural to use different time steps in different subdomains and we apply the projection algorithm in [13] adapted to time discretizations to exchange information on the space-time interfaces, for the lowest order DG method in time. We show the numerical behaviour of both methods for different test cases suggested by ANDRA for the simulation of underground nuclear waste storage. A preliminary version of this work was given in [19].

The remainder of this paper is organized as follows: in the next section we present the model problem in a mixed formulation. We prove its well-posedness for Dirichlet and Robin boundary conditions in Section 3. In Section 4, we introduce the equivalent multidomain problem using nonoverlapping domain decomposition and describe the two solution methods. A convergence proof for the OSWR algorithm for the mixed formulation is given. In Section 5, we consider the semi-discrete problems in time using different time grids in the subdomains. In section 6, results of 2D numerical experiments showing that the methods preserve the order of the global scheme are discussed.

2. A model problem. In this section we define our model problem and show the existence and uniqueness of its solution. For an open, bounded domain Ω of $\mathbb{R}^d$ $(d = 2, 3)$ with Lipschitz boundary $\partial\Omega$ and some fixed time $T > 0$, we consider the following time-dependent diffusion problem

$$\omega \partial_t c + \nabla \cdot (-\boldsymbol{D} \nabla c) = f, \quad \text{in } \Omega \times (0, T), \tag{2.1}$$

with boundary and initial conditions

$$\begin{aligned} c &= 0, \quad \text{on } \partial\Omega \times (0, T), \\ c(\cdot, 0) &= c_0, \quad \text{in } \Omega. \end{aligned} \tag{2.2}$$

Here c is the concentration of a contaminant dissolved in a fluid, f the source term, ω the porosity and $\boldsymbol{D}$ a symmetric time independent diffusion tensor. We assume that ω is bounded above and below by positive constants, $0 < \omega_- \leq \omega(x) \leq \omega_+$, and that there exists δ_- and δ_+ positive constants such that $\xi^T \boldsymbol{D}^{-1}(x)\xi \geq \delta_- |\xi|^2$, and $|\boldsymbol{D}(x)\xi| \leq \delta_+ |\xi|$, for a.e. $x \in \Omega$ and $\forall \xi \in \mathbb{R}^d$. For simplicity, we have imposed a homogeneous Dirichlet boundary condition on $\partial\Omega$. In practice, we may use non-homogeneous Dirichlet and Neumann boundary conditions for which the analysis remains valid (see Section 3 for the extension to Robin boundary conditions).

We now rewrite (2.1) in an equivalent mixed form by introducing the vector field $\boldsymbol{r} := -\boldsymbol{D}\nabla c$. This yields

$$\begin{aligned} \omega\partial_t c + \nabla\cdot\boldsymbol{r} &= f, \quad \text{in } \Omega\times(0,T)\,, \\ \nabla c + \boldsymbol{D}^{-1}\boldsymbol{r} &= 0, \quad \text{in } \Omega\times(0,T)\,. \end{aligned} \tag{2.3}$$

To write the variational formulation for (2.3) (see [5, 30]), we introduce the spaces

$$M = L^2(\Omega) \ \text{ and } \ \Sigma = H(\mathrm{div},\Omega)\,.$$

We multiply the first and second equations in (2.3) by $\mu\in M$ and $\boldsymbol{v}\in\Sigma$ respectively, then integrate over Ω and apply Green's formula to obtain:

For a.e. $t\in(0,T)$, find $c(t)\in M$ and $\boldsymbol{r}(t)\in\Sigma$ such that

$$\begin{aligned} \frac{d}{dt}(\omega c,\mu) + (\nabla\cdot\boldsymbol{r},\mu) &= (f,\mu), \quad \forall\mu\in M, \\ -(\nabla\cdot\boldsymbol{v},c) + (\boldsymbol{D}^{-1}\boldsymbol{r},\boldsymbol{v}) &= 0, \qquad\quad \forall\boldsymbol{v}\in\Sigma, \end{aligned} \tag{2.4}$$

together with initial condition (2.2).

Here and in the following, we will use the convention that if V is a space of functions, then we write $\boldsymbol{V}$ for a space of vector functions having each component in V. We also denote by $(\cdot,\cdot)$ the inner product in $L^2(\Omega)$ or $\boldsymbol{L^2(\Omega)}$ and $\|\cdot\|$ the $L^2(\Omega)$-norm or $\boldsymbol{L^2(\Omega)}$-norm.

The well-posedness of problem (2.4) is shown in in [23, 4], with an argument based on a Galerkin's method and a priori estimates:

THEOREM 2.1. *If f is in $L^2(0,T;L^2(\Omega))$ and c_0 in $H^1_0(\Omega)$ then problem* (2.4)*,* (2.2) *has a unique solution*

$$(c,\boldsymbol{r})\in H^1(0,T;L^2(\Omega))\times\left(L^2(0,T;H(\mathrm{div},\Omega))\cap L^\infty(0,T;\boldsymbol{L^2(\Omega)})\right).$$

Moreover, if $\boldsymbol{D}$ is in $\boldsymbol{W^{1,\infty}(\Omega)}$, f in $H^1(0,T;L^2(\Omega))$ and c_0 in $H^2(\Omega)\cap H^1_0(\Omega)$ then

$$(c,\boldsymbol{r})\in W^{1,\infty}(0,T;L^2(\Omega))\times\left(L^\infty(0,T;H(\mathrm{div},\Omega))\cap H^1(0,T;\boldsymbol{L^2(\Omega)})\right).$$

Remark. We give the proof of Theorem thrm1 in the finite dimensional setting since some technical points (those involving $\partial_t\boldsymbol{r}$, or $\mathbf{r}$ at time $t=0$) can only be defined by their finite dimensional Galerkin approximation. This is not surprising given the differential-algebraic structure of system (3.2): the second equation has no time derivative. In DAE theory it is well known that the algebraic equations have to be differentiated a number of times (this is what defines the index), and that this imposes compatibility conditions between the initial data (note that $\boldsymbol{r}(0)$ is not given). The index has been extended to PDEs, see for instance [27].

The proof of Theorem 2.1 is carried out in several steps: in Lemma 2.2 we first construct solutions of certain finite-dimensional approximations of (2.4), then we derive suitable energy estimates in Lemma 2.3 and prove the first part of the theorem. The higher regularity of the solution is obtained from the estimates given in Lemma 2.4.

We need first to introduce some notations: Let $\{\mu_n \mid n\in\mathbb{N}\}$ be a Hilbert basis of M and $\{\boldsymbol{v}_n \mid n\in\mathbb{N}\}$ be a Hilbert basis of Σ. For each pair of positive integers n and m, we denote by M_n the finite dimensional subspace spanned by $\{\mu_i\}_{i=1}^n$, and Σ_m the finite dimensional subspace spanned by $\{\boldsymbol{v}_i\}_{i=1}^m$. Now let $c_n:[0,T]\to M_n$ and $\boldsymbol{r}_m:[0,T]\to\Sigma_m$ be the solution of the following problem

$$\begin{aligned} (\omega\partial_t c_n,\mu_i) + (\nabla\cdot\boldsymbol{r}_m,\mu_i) &= (f(t),\mu_i), \quad \forall i=1,\dots,n, \\ -(\nabla\cdot\boldsymbol{v}_j,c_n) + (\boldsymbol{D}^{-1}\boldsymbol{r}_m,\boldsymbol{v}_j) &= 0, \qquad\qquad \forall j=1,\dots,m, \end{aligned} \tag{2.5}$$

with

$$(c_n(0), \mu_i) = (c_0, \mu_i), \quad \forall i = 1, \ldots, n. \tag{2.6}$$

LEMMA 2.2. (Construction of approximate solutions) *For each pair* $(n, m) \in \mathbb{N}^2$, $n, m \geq 1$, *there exists a unique solution* $(c_n, \boldsymbol{r}_m)$ *to problem* (2.5).

Proof. We introduce the following notations

$(\boldsymbol{F}_n(t))_i = (f(t), \mu_i)$, $(\boldsymbol{C}_0)_i = (c_0, \mu_i)$, $(\boldsymbol{W}_n)_{ij} = (\omega\mu_j, \mu_i)$, $\forall\, 1 \leq i, j \leq n$,

$(\boldsymbol{A}_m)_{ij} = (\boldsymbol{D}^{-1}\boldsymbol{v}_j, \boldsymbol{v}_i)$, $\forall\, 1 \leq i, j \leq m$, $(\boldsymbol{B}_{nm})_{ij} = (\nabla \cdot \boldsymbol{v}_j, \mu_i)$, $\forall\, 1 \leq i \leq n, 1 \leq j \leq m$.

We also denote by $\boldsymbol{C}_n(t)$ the vector of degrees of freedom of $c_n(t)$ with respect to the basis $\{\mu_i\}_{i=1}^n$ and $\boldsymbol{R}_m(t)$ that of $\boldsymbol{r}_m(t)$ with respect to the basis $\{\boldsymbol{v}_i\}_{i=1}^m$. With this notation, (2.5) may be rewritten as

$$\boldsymbol{W}_n \frac{d\boldsymbol{C}_n}{dt}(t) + \boldsymbol{B}_{nm}\boldsymbol{R}_m(t) = \boldsymbol{F}_n(t), \tag{2.7a}$$

$$-\boldsymbol{B}_{nm}^T\boldsymbol{C}_n(t) + \boldsymbol{A}_m\boldsymbol{R}_m(t) = 0, \tag{2.7b}$$

$$\boldsymbol{C}_n(0) = \boldsymbol{C}_0. \tag{2.7c}$$

As $\boldsymbol{A}_m$ is a symmetric and positive definite square matrix of size m (because of the assumptions concerning $\boldsymbol{D}$), $\boldsymbol{A}_m$ is invertible. Thus (2.7b) implies

$$\boldsymbol{R}_m(t) = \boldsymbol{A}_m^{-1}\boldsymbol{B}_{nm}^T\boldsymbol{C}_n(t). \tag{2.8}$$

Substituting (2.8) into (2.7a) and as $\boldsymbol{W}_n$ is invertible, we obtain

$$\frac{d\boldsymbol{C}_n}{dt}(t) + \boldsymbol{W}_n^{-1}\boldsymbol{B}_{nm}\boldsymbol{A}_m^{-1}\boldsymbol{B}_{nm}^T\boldsymbol{C}_n(t) = \boldsymbol{W}_n^{-1}\boldsymbol{F}_n(t), \quad \text{for a.e. } t \in [0, T]. \tag{2.9}$$

This is a system of n linear ODEs of order 1 with initial condition (2.7c). Hence, there exists a unique function $\boldsymbol{C}_n \in (C([0,T]))^n$ with $\dfrac{d\boldsymbol{C}_n}{dt} \in \left(L^2(0,T)\right)^n$ satisfying (2.9) and (2.7c) (see [8]). From (2.8) we obtain $\boldsymbol{R}_m \in (C([0,T]))^m$ such that $\dfrac{d\boldsymbol{R}_m}{dt} \in \left(L^2(0,T)\right)^m$ and then $(c_n, \boldsymbol{r}_m)$, which is the unique solution to (2.5). ∎

In the next step, we derive some suitable a priori estimates similar to those given in [23] but in a more detailed manner.

LEMMA 2.3. *There exists a constant C independent of n and m such that*

$$\begin{aligned}\|c_n\|_{L^\infty(0,T;L^2(\Omega))} + \|\partial_t c_n\|_{L^2(0,T;L^2(\Omega))} + \|\boldsymbol{r}_m\|_{L^\infty(0,T;\mathbf{L}^2(\Omega))} + \|\boldsymbol{r}_m\|_{L^2(0,T;H(\mathrm{div},\Omega))} \\ \leq C(\|c_0\|_{H_0^1(\Omega)} + \|f\|_{L^2(0,T;L^2(\Omega))}), \quad \forall n, m \geq 1.\end{aligned}$$

Proof. We prove this lemma by deriving successively the estimates on c_n, $\partial_t c_n$ and $\boldsymbol{r}_m$, and finally on $\nabla \cdot \boldsymbol{r}_m$ for the $H(\mathrm{div}, \Omega)$-norm.

• Let $n, m \geq 1$ and take $c_n(t) \in M_n$ and $\boldsymbol{r}_m(t) \in \Sigma_m$ as the test functions in (2.5)

$$\begin{aligned}(\omega\partial_t c_n, c_n) + (\nabla \cdot \boldsymbol{r}_m, c_n) &= (f, c_n), \\ -(\nabla \cdot \boldsymbol{r}_m, c_n) + (\boldsymbol{D}^{-1}\boldsymbol{r}_m, \boldsymbol{r}_m) &= 0.\end{aligned}$$

Adding these two equations, we obtain

$$(\omega\partial_t c_n, c_n) + (\boldsymbol{D}^{-1}\boldsymbol{r}_m, \boldsymbol{r}_m) = (f, c_n).$$

Using the properties of ω and $\boldsymbol{D}$, and applying the Cauchy-Schwarz inequality, we get

$$(\omega\partial_t c_n, c_n) = \frac{1}{2}\frac{d}{dt}(\omega c_n(t), c_n(t)) \geq \frac{\omega_-}{2}\frac{d}{dt}\|c_n(t)\|^2,$$
$$(\boldsymbol{D}^{-1}\boldsymbol{r}_m(t), \boldsymbol{r}_m(t)) \geq \delta_- \|\boldsymbol{r}_m(t)\|,$$
$$(f(t), c_n(t)) \leq \|f(t)\|\,\|c_n(t)\| \leq \frac{1}{2\omega_-}\|f(t)\|^2 + \frac{\omega_-}{2}\|c_n(t)\|^2.$$

As $\omega_- > 0$, we deduce that

$$\frac{d}{dt}\|c_n(t)\|^2 + \frac{2\delta_-}{\omega_-}\|\boldsymbol{r}_m(t)\|^2 \leq \frac{1}{\omega_-^2}\|f(t)\|^2 + \|c_n(t)\|^2.$$

Integrating this inequality over $(0,t)$ for $t \in [0,T]$, we find

$$\|c_n(t)\|^2 + \frac{2\delta_-}{\omega_-}\int_0^t \|\boldsymbol{r}_m(s)\|^2 ds \leq \|c(0)\|^2 + \frac{1}{\omega_-^2}\int_0^t \|f(s)\|^2 ds + \int_0^t \|c_n(s)\|^2 ds, \quad (2.10)$$

since $\|c_n(0)\|^2 = \sum_{i=1}^{n}(c_0,\mu_i)^2 \leq \sum_{i=1}^{\infty}(c_0,\mu_i)^2 = \|c_0\|^2$.

Thus (2.10) implies

$$\|c_n(t)\|^2 \leq (\|c_0\|^2 + \frac{1}{\omega_-^2}\|f\|^2_{L^2(0,T;L^2(\Omega))}) + \int_0^t \|c_n(s)\|^2 ds.$$

Applying Gronwall's lemma, there exists C independent of n or m such that

$$\|c_n\|^2_{L^\infty(0,T;L^2(\Omega))} \leq C(\|c_0\|^2 + \|f\|^2_{L^2(0,T;L^2(\Omega))}), \quad (2.11)$$

• Now we derive the estimate for $\partial_t c_n$: Taking $\partial_t c_n \in M_n$ as the test function in the first equation of (2.5), we obtain

$$(\omega\partial_t c_n, \partial_t c_n) + (\nabla\cdot\boldsymbol{r}_m, \partial_t c_n) = (f, \partial_t c_n). \quad (2.12)$$

Differentiating the second equation of (2.5) with respect to t, we find

$$-(\nabla\cdot\boldsymbol{v}, \partial_t c_n) + (\boldsymbol{D}^{-1}\partial_t\boldsymbol{r}_m, \boldsymbol{v}) = 0, \quad \forall \boldsymbol{v} \in \Sigma_m. \quad (2.13)$$

Then we take $\boldsymbol{r}_m$ as the test function in (2.13)

$$(\boldsymbol{D}^{-1}\partial_t\boldsymbol{r}_m, \boldsymbol{r}_m) - (\nabla\cdot\boldsymbol{r}_m, \partial_t c_n) = 0. \quad (2.14)$$

Adding (2.12) and (2.14), we see that

$$(\omega\partial_t c_n, \partial_t c_n) + (\boldsymbol{D}^{-1}\partial_t\boldsymbol{r}_m, \boldsymbol{r}_m) = (f, \partial_t c_n).$$

As $\boldsymbol{D}$ is symmetric and positive definite, by applying the Cauchy-Schwarz inequality to the right hand side as well as using the property of ω, we obtain

$$\omega_-\|\partial_t c_n(t)\|^2 + \frac{d}{dt}\|\sqrt{\boldsymbol{D}^{-1}}\boldsymbol{r}_m(t)\|^2 \leq \frac{1}{\omega_-}\|f(t)\|^2. \quad (2.15)$$

Integrating (2.15) over $(0,t)$ for $t \in [0,T]$, we find

$$\omega_- \int_0^t \|\partial_t c_n(s)\|^2 ds + \|\sqrt{\boldsymbol{D}^{-1}}\boldsymbol{r}_m(t)\|^2 \le \|\sqrt{\boldsymbol{D}^{-1}}\boldsymbol{r}_m(0)\|^2 + \frac{1}{\omega_-}\int_0^t \|f(s)\|^2 ds. \quad (2.16)$$

To bound $\|\boldsymbol{r}_m(0)\|$, we take $\boldsymbol{r}_m \in \Sigma_m$ as the test function in the second equation of (2.5) and let $t=0$

$$(\boldsymbol{D}^{-1}\boldsymbol{r}_m(0), \boldsymbol{r}_m(0)) = (\nabla \cdot \boldsymbol{r}_m(0), c_n(0)). \quad (2.17)$$

Noting that (2.17) holds for all $n, m \ge 1$, we bound the left-hand side as before and let $n \to \infty$. Since $c_n(0) \to c_0$ in $L^2(\Omega)$ and $c_0 \in H_0^1(\Omega)$, we have by Green's formula

$$\delta_- \|\boldsymbol{r}_m(0)\|^2 \le (\nabla \cdot \boldsymbol{r}_m(0), c_0) = (\boldsymbol{r}_m(0), -\nabla c_0) \le \|\boldsymbol{r}_m(0)\| \, \|\nabla c_0\|.$$

Thus

$$\|\boldsymbol{r}_m(0)\| \le C\|c_0\|_{H_0^1(\Omega)}. \quad (2.18)$$

This along with (2.16) yields

$$\|\partial_t c_n\|^2_{L^2(0,T;L^2(\Omega))} + \|\boldsymbol{r}_m\|^2_{L^\infty(0,T;\mathbf{L^2(\Omega)})} \le C(\|c_0\|^2_{H_0^1(\Omega)} + \|f\|^2_{L^2(0,T;L^2(\Omega))}), \ \forall n, m \ge 1. \quad (2.19)$$

There only remains to show that $\|\nabla \cdot \boldsymbol{r}_m\|_{L^2(0,T;\mathbf{L^2(\Omega)})}$ is bounded.

• Fixing $m \ge 1$, as $\nabla \cdot \boldsymbol{r}_m(t) \in M$ we can write

$$\nabla \cdot \boldsymbol{r}_m(t) = \sum_{i=1}^{\infty} \xi_m^i(t)\mu_i, \text{ for a.e. } t \in (0,T), \quad (2.20)$$

where $\xi_m^i(t) = (\nabla \cdot \boldsymbol{r}_m(t), \mu_i)$. Now we fix $n \ge 1$ and multiply the first equation of (2.5) by $\xi_m^i(t)$, sum over $i = 1, \ldots, n$, we see that

$$(\nabla \cdot \boldsymbol{r}_m, \sum_{i=1}^n \xi_m^i \mu_i) \le \frac{1}{2}(\|f\| + C\|\partial_t c_n\|)^2 + \frac{1}{2}\|\sum_{i=1}^n \xi_m^i \mu_i\|^2. \quad (2.21)$$

Integrating with respect to time and recalling (2.19), we find

$$\int_0^T (\nabla \cdot \boldsymbol{r}_m, \sum_{i=1}^n \xi_m^i \mu_i) dt \le C(\|f\|^2_{L^2(0,T;L^2(\Omega))} + \|c_0\|^2_{H_0^1(\Omega)}) + \frac{1}{2}\int_0^T \|\sum_{i=1}^n \xi_m^i \mu_i\|^2 dt.$$

Let $n \to \infty$ and recall (2.20), we obtain

$$\int_0^T \|\nabla \cdot \boldsymbol{r}_m\|^2 dt \le C(\|f\|^2_{L^2(0,T;L^2(\Omega))} + \|c_0\|^2_{H_0^1(\Omega)}) + \frac{1}{2}\int_0^T \|\nabla \cdot \boldsymbol{r}_m\|^2 dt.$$

Thus

$$\|\nabla \cdot \boldsymbol{r}_m\|^2_{L^2(0,T;L^2(\Omega))} \le C(\|f\|^2_{L^2(0,T;L^2(\Omega))} + \|c_0\|^2_{H_0^1(\Omega)}).$$

On the other hand, by recalling inequality (2.10) with $t = T$ and by (2.11), we find

$$\|\boldsymbol{r}_m\|^2_{L^2(0,T;\mathbf{L^2(\Omega)})} \le C(\|c_0\|^2 + \|f\|^2_{L^2(0,T;L^2(\Omega))}).$$

Hence,

$$\begin{aligned}\|\boldsymbol{r}_m\|^2_{L^2(0,T;H(\mathrm{div},\Omega))} &= \|\boldsymbol{r}_m\|^2_{L^2(0,T;(L^2(\Omega))^2)} + \|\nabla\cdot\boldsymbol{r}_m\|^2_{L^2(0,T;L^2(\Omega))}\\ &\le C(\|f\|^2_{L^2(0,T;L^2(\Omega))} + \|c_0\|^2_{H^1_0(\Omega)}), \quad \forall m \ge 1,\end{aligned}$$

which ends the proof of Lemma 2.3. □

We now prove the first part of Theorem 2.1: there exists a unique solution $(c, \boldsymbol{r})$ in $H^1(0,T;L^2(\Omega)) \times L^2(0,T;H(div,\Omega)) \cap L^\infty(0,T;\mathbf{L^2(\Omega)})$ of problem (2.3).

Proof. The proof of the first part of Theorem 2.1 follows the following steps:.

• Lemma 2.3 implies that for the sequences $\{c_n\}_{n=1}^\infty$ and $\{\boldsymbol{r}_m\}_{m=1}^\infty$ defined by (2.5) and (2.6), $\{c_n\}_{n=1}^\infty$ is bounded in $L^2(0,T;L^2(\Omega))$, $\{\partial_t c_n\}_{n=1}^\infty$ is bounded in $L^2(0,T;L^2(\Omega))$ and $\{\boldsymbol{r}_m\}_{m=1}^\infty$ is bounded in $L^2(0,T;H(\mathrm{div},\Omega)) \cap L^\infty(0,T;\mathbf{L^2(\Omega)})$. Thus, there exist subsequences, still denoted by $\{c_n\}_{n=1}^\infty$ and $\{\boldsymbol{r}_m\}_{m=1}^\infty$ and functions $c \in L^2(0,T;L^2(\Omega))$ with $\partial_t c \in L^2(0,T;L^2(\Omega))$ and $\boldsymbol{r} \in L^2(0,T;H(\mathrm{div},\Omega)) \cap L^\infty(0,T;\mathbf{L^2(\Omega)})$ such that

$$\begin{aligned}&c_n \rightharpoonup c \text{ in } L^2(0,T;L^2(\Omega)),\\ &\partial_t c_n \rightharpoonup \partial_t c \text{ in } L^2(0,T;L^2(\Omega)),\\ &\boldsymbol{r}_m \rightharpoonup \boldsymbol{r} \text{ in } L^2(0,T;H(\mathrm{div},\Omega)).\end{aligned} \tag{2.22}$$

• Next let $\eta \in C^1([0,T];M_{n_0})$, $\boldsymbol{w} \in C^1([0,T];\Sigma_{m_0})$ for $n_0, m_0 \ge 1$. We choose $n \ge n_0$ and $m \ge m_0$, take η and $\boldsymbol{w}$ as the test functions in (2.5) and then integrate with respect to time

$$\begin{aligned}\int_0^T (\omega\partial_t c_n, \eta) + (\nabla\cdot\boldsymbol{r}_m, \eta)dt &= \int_0^T (f,\eta)dt,\\ \int_0^T -(\nabla\cdot\boldsymbol{w}, c_n) + (\boldsymbol{D}^{-1}\boldsymbol{r}_m, \boldsymbol{w})dt &= 0.\end{aligned} \tag{2.23}$$

Because of the weak convergence in (2.22), we also have

$$\begin{aligned}\int_0^T (\omega\partial_t c, \eta) + (\nabla\cdot\boldsymbol{r}, \eta)dt &= \int_0^T (f,\eta)dt,\\ \int_0^T -(\nabla\cdot\boldsymbol{w}, c) + (\boldsymbol{D}^{-1}\boldsymbol{r}, \boldsymbol{w})dt &= 0.\end{aligned} \tag{2.24}$$

Since the spaces of test functions $\eta, \boldsymbol{w}$ are dense in $L^2(0,T;M)$ and $L^2(0,T;\Sigma)$ respectively, it follows from (2.24) that (2.4) holds for a.e. $t \in (0,T)$ (see [8]).

• There remains to show that $c(0) = c_0$. Toward this end, we take $\eta \in C^1([0,T];M_{n_0})$ with $\eta(T) = 0$. It follows from the first equation of (2.24) that

$$-\int_0^T (\omega\partial_t\eta, c) + (\nabla\cdot\boldsymbol{r}, \eta)dt = \int_0^T (f,\eta)dt + (\omega c(0), \eta(0)). \tag{2.25}$$

Similarly, from the first equation of (2.23) we deduce

$$-\int_0^T (\omega\partial_t\eta, c_n) + (\nabla\cdot\boldsymbol{r}_m, \eta)dt = \int_0^T (f,\eta)dt + (\omega c_n(0), \eta(0)).$$

Using (2.22), we obtain

$$-\int_0^T (\omega\partial_t\eta, c) + (\nabla\cdot\boldsymbol{r}, \eta)dt = \int_0^T (f,\eta)dt + (\omega c_0, \eta(0)), \tag{2.26}$$

since $c_n(0) \to c_0$ in $L^2(\Omega)$. As $\eta(0)$ is arbitrary, by comparing (2.25) and (2.26) we conclude that $c(0) = c_0$.

• For the uniqueness, as the equations are linear, it suffices to check that $c = 0$ and $\boldsymbol{r} = 0$ for $f = 0$ and $c_0 = 0$. To prove this, we set $\mu = c$ and $\boldsymbol{v} = \boldsymbol{r}$ in (2.4) (for $f = 0$) and add the two resulting equations:

$$\frac{1}{2}\frac{d}{dt}(\omega c, c) + (\boldsymbol{D}^{-1}\boldsymbol{r}, \boldsymbol{r}) = 0.$$

Using the property of ω and the fact that $(\boldsymbol{D}^{-1}\boldsymbol{r}, \boldsymbol{r}) \geq \delta_- \|\boldsymbol{r}\|^2 \geq 0$, then integrating with respect to t we see that

$$\omega_- \|c(t)\|^2 + 2\delta_- \int_0^t \|\boldsymbol{r}(s)\|^2_{\mathbf{L^2(\Omega)}} ds \leq 0, \quad \text{for a.e. } t \in (0,T),$$

where $c(0) = c_0 = 0$. Thus $c = 0$ and $\boldsymbol{r} = 0$ for a.e. $t \in (0,T)$. ∎

We now prove the second part of Theorem 2.1. The higher regularity of the solution to (2.3) is obtained by using the following lemma.

LEMMA 2.4. (Estimates for improved regularity) *Assume that $\boldsymbol{D}$ is in $\boldsymbol{W^{1,\infty}(\Omega)}$, c_0 in $H^2(\Omega) \cap H_0^1(\Omega)$ and f in $H^1(0,T;L^2(\Omega))$ then*

$$\|\partial_t c\|_{L^\infty(0,T;L^2(\Omega))} + \|\boldsymbol{r}\|_{L^\infty(0,T;H(\mathrm{div},\Omega))} + \|\partial_t \boldsymbol{r}\|_{L^2(0,T;\mathbf{L^2(\Omega)})} \leq C(\|f\|_{H^1(0,T;L^2(\Omega))} + \|c_0\|_{H^2(\Omega)}).$$

Proof. As $f \in H^1(0,T;L^2(\Omega))$, the solutions of the ODE system (2.7) are more regular in time than before (i.e. up to second-order time derivatives).

Let $n, m \geq 1$. First, we differentiate the first equation of (2.5) with respect to t

$$(\omega \partial_{tt} c_n, \mu_i) + (\nabla \cdot \partial_t \boldsymbol{r}_m, \mu_i) = (\partial_t f, \mu_i), \quad \forall i = 1, \dots, n,$$

then we take $\partial_t c_n$ as the test function

$$(\omega \partial_{tt} c_n, \partial_t c_n) + (\nabla \cdot \partial_t \boldsymbol{r}_m, \partial_t c_n) = (\partial_t f, \partial_t c_n). \tag{2.27}$$

Similarly, we differentiate the second equation of (2.5) with respect to t

$$(\boldsymbol{D}^{-1}\partial_t \boldsymbol{r}_m, \boldsymbol{v}_i) - (\nabla \cdot v_i, \partial_t c_n) = 0, \quad \forall i = 1, \dots, m,$$

and take $\partial_t \boldsymbol{r}_m$ as the test function

$$(\boldsymbol{D}^{-1}\partial_t \boldsymbol{r}_m, \partial_t \boldsymbol{r}_m) - (\nabla \cdot \partial_t \boldsymbol{r}_m, \partial_t c_n) = 0. \tag{2.28}$$

Adding (2.27) and (2.28), we find

$$(\omega \partial_{tt} c_n, \partial_t c_n) + (\boldsymbol{D}^{-1}\partial_t \boldsymbol{r}_m, \partial_t \boldsymbol{r}_m) = (\partial_t f, \partial_t c_n).$$

Bounding $(\boldsymbol{D}^{-1}\partial_t \boldsymbol{r}_m, \partial_t \boldsymbol{r}_m) \geq \delta_- \|\partial_t \boldsymbol{r}_m\|^2$, using the assumption about ω and applying the Cauchy-Schwarz inequality, we obtain

$$\frac{d}{dt}\|\partial_t c_n\|^2 + \frac{2\delta_-}{\omega_-}\|\partial_t \boldsymbol{r}_m\|^2 \leq \frac{1}{\omega_-^2}\|\partial_t f\|^2 + \|\partial_t c_n\|^2.$$

For each $t \in [0,T]$, we may integrate over $(0,t)$ to obtain

$$\|\partial_t c_n(t)\|^2 + \frac{2\delta_-}{\omega_-}\int_0^t \|\partial_t \boldsymbol{r}_m\|^2 ds \leq \|\partial_t c_n(0)\|^2 + \frac{1}{\omega_-^2}\int_0^t \|\partial_t f\|^2 ds + \int_0^t \|\partial_t c_n\|^2 ds. \tag{2.29}$$

In order to bound $\|\partial_t c_n(0)\|$, we use the first equation of (2.5) (with $\partial_t c_n$ as the test function, at $t=0$) to obtain

$$\|\partial_t c_n(0)\| \leq C(\|\nabla \cdot \boldsymbol{r}_m(0)\| + \|f(0)\|).$$

Using the second equation of (2.5) at $t=0$, and then let $n \to \infty$ to get

$$(\boldsymbol{D}^{-1}\boldsymbol{r}_m(0) + \nabla c_0, \boldsymbol{v}) = 0, \quad \forall \boldsymbol{v} \in \Sigma_m.$$

Thus, using density argument and $c_0 \in H_0^1(\Omega) \cap H^2(\Omega)$, we obtain $\boldsymbol{D}^{-1}\boldsymbol{r}_m(0) = -\nabla c_0$ in $H^1(\Omega)$. Then, we bound

$$\|\partial_t c_n(0)\|^2 \leq C(\|c_0\|^2_{H^2(\Omega)} + \|f(0)\|^2). \tag{2.30}$$

Replacing (2.30) in (2.29), we obtain

$$\begin{aligned}\|\partial_t c_n(t)\|^2 + \frac{2\delta_-}{\omega_-}\int_0^t \|\partial_t \boldsymbol{r}_m\|^2 ds \\ \leq C(\|c_0\|^2_{H^2(\Omega)} + \|f\|^2_{H^1(0,T;L^2(\Omega))}) + \int_0^t \|\partial_t c_n\|^2 ds.\end{aligned} \tag{2.31}$$

It now follows from (2.31) and Gronwall's lemma that

$$\|\partial_t c_n\|^2_{L^\infty(0,T;L^2(\Omega))} + \frac{2\delta_-}{\omega_-}\|\partial_t \boldsymbol{r}_m\|^2_{L^2(0,T;\mathbf{L^2(\Omega)})} \leq C(\|c_0\|^2_{H^2(\Omega)} + \|f\|^2_{H^1(0,T;L^2(\Omega))}). \tag{2.32}$$

Recalling (2.21) and using (2.32), we obtain

$$(\nabla \cdot \boldsymbol{r}_m, \sum_{i=1}^n \xi_m^i \mu_i) \leq C(\|c_0\|^2_{H^2(\Omega)} + \|f\|^2_{H^1(0,T;L^2(\Omega))}) + \frac{1}{2}\|\sum_{i=1}^n \xi_m^i \mu_i\|^2.$$

Then, let $n \to \infty$, we see that

$$\|\nabla \cdot \boldsymbol{r}_m\|^2_{L^\infty(0,T;L^2(\Omega))} \leq C(\|c_0\|^2_{H^2(\Omega)} + \|f\|^2_{H^1(0,T;L^2(\Omega))}).$$

This along with (2.19) gives

$$\|\boldsymbol{r}_m\|^2_{L^\infty(0,T;H(\mathrm{div},\Omega))} \leq C(\|c_0\|^2_{H^2(\Omega)} + \|f\|^2_{H^1(0,T;L^2(\Omega))}). \tag{2.33}$$

The lemma now follows from (2.32), (2.33) and (2.22). $\square$

In the sequel, we will consider two domain decomposition methods for solving (2.4), (2.2). The first one involves local Dirichlet subproblems whose well-posedness is an extension of Theorem 2.1. In the second approach, the optimized Schwarz waveform relaxation method, we shall impose Robin transmission conditions on the interfaces. Thus, we extend the well-posedness results above to the case of Robin boundary conditions.

3. A local problem with Robin boundary conditions. In this section, we consider problem (2.1)-(2.2) with Robin boundary conditions on $\partial\Omega \times (0,T)$:

$$-\boldsymbol{r}\cdot\boldsymbol{n} + \alpha c = g, \quad \text{on } \partial\Omega \times (0,T), \tag{3.1}$$

where α defined on $\partial\Omega$ is a time independent positive, bounded coefficient and g is a space-time function. We define $\breve{\alpha} := \dfrac{1}{\alpha}$ and suppose that $0 < \kappa_1 \le \breve{\alpha} \le \kappa_2$ a.e. in $\partial\Omega$. We denote by $(\cdot,\cdot)_{\partial\Omega}$ and $\|\cdot\|_{\partial\Omega}$ the inner product and norm in $L^2(\partial\Omega)$ respectively. To derive a variational formulation corresponding to boundary condition (3.1), we introduce the following Hilbert space

$$\widetilde{\Sigma} = \mathcal{H}(\mathrm{div},\Omega) := \{\boldsymbol{v} \in H(\mathrm{div},\Omega) |\ \boldsymbol{v}\cdot\boldsymbol{n} \in L^2(\partial\Omega)\},$$

equipped with the norm

$$\|\boldsymbol{v}\|^2_{\mathcal{H}(\mathrm{div},\Omega)} := \|\boldsymbol{v}\|_{H(\mathrm{div},\Omega)} + \|\boldsymbol{v}\cdot\boldsymbol{n}\|^2_{\partial\Omega}.$$

The weak problem with Robin boundary conditions may now be written as follows:

For a.e. $t \in (0,T)$, find $c(t) \in M$ and $\boldsymbol{r}(t) \in \widetilde{\Sigma}$ such that

$$\begin{aligned} (\omega\partial_t c,\mu) + (\nabla\cdot\boldsymbol{r},\mu) \quad &= (f,\mu), && \forall \mu \in M,\\ -(\nabla\cdot\boldsymbol{v},c) + (\boldsymbol{D}^{-1}\boldsymbol{r},\boldsymbol{v}) + (\breve{\alpha}\boldsymbol{r}\cdot\boldsymbol{n},\boldsymbol{v}\cdot\boldsymbol{n})_{\partial\Omega} \quad &= -(\breve{\alpha}g,\boldsymbol{v}\cdot\boldsymbol{n})_{\partial\Omega}, && \forall \boldsymbol{v} \in \widetilde{\Sigma}. \end{aligned} \tag{3.2}$$

THEOREM 3.1. *If f is in $L^2(0,T;L^2(\Omega))$, g in $H^1(0,T;L^2(\partial\Omega))$ and c_0 in $H^1(\Omega)$, then problem (3.2), (2.2) has a unique solution*

$$(c,\boldsymbol{r}) \in\ H^1(0,T;L^2(\Omega)) \times \left(L^2(0,T;\mathcal{H}(\mathrm{div},\Omega)) \cap L^\infty(0,T;\boldsymbol{L^2(\Omega)})\right).$$

Moreover, if $\boldsymbol{D}$ is in $\boldsymbol{W^{1,\infty}(\Omega)}$, f in $H^1(0,T;L^2(\Omega))$ and c_0 in $H^2(\Omega)$ then

$$(c,\boldsymbol{r}) \in\ W^{1,\infty}(0,T;L^2(\Omega)) \times \left(L^\infty(0,T;\mathcal{H}(\mathrm{div},\Omega)) \cap H^1(0,T;\boldsymbol{L^2(\Omega)})\right).$$

Proof. The proof of Theorem 3.1 relies on energy estimates and Gronwall's lemma, together with a Galerkin method, as for the proof of Theorem 2.1. We only present here parts of the proof that are different from those of the proof of Theorem 2.1. We construct the finite-dimensional approximation problems to (3.2) as follows

$$\begin{aligned} (\omega\partial_t c_n,\mu_i) + (\nabla\cdot\boldsymbol{r}_m,\mu_i) \ &= (f,\mu_i), && 1 \le i \le n,\\ -(\nabla\cdot\tilde{\boldsymbol{v}}_j,c_n) + (\boldsymbol{D}^{-1}\boldsymbol{r}_m,\tilde{\boldsymbol{v}}_j) + (\breve{\alpha}\boldsymbol{r}_m\cdot\boldsymbol{n},\tilde{\boldsymbol{v}}_j\cdot\boldsymbol{n})_{\partial\Omega} \ &= (-\breve{\alpha}g,\tilde{\boldsymbol{v}}_j\cdot\boldsymbol{n})_{\partial\Omega}, && 1 \le j \le m, \end{aligned} \tag{3.3}$$

where $c_n \in M_n$, $\boldsymbol{r}_m \in \widetilde{\Sigma}_m$ and $\tilde{\boldsymbol{v}}_i, i = 1,\ldots,m$ is the basis of $\widetilde{\Sigma}_m$. We then rewrite (3.3) in matrix form as in (2.7):

$$\begin{aligned} \boldsymbol{W}_n\frac{d\boldsymbol{C}_n}{dt}(t) + \tilde{\boldsymbol{B}}_{nm}\tilde{\boldsymbol{R}}_m(t) \ &= \boldsymbol{F}_n(t),\\ -\tilde{\boldsymbol{B}}^T_{nm}\boldsymbol{C}_n(t) + \tilde{\boldsymbol{A}}_m\tilde{\boldsymbol{R}}_m(t) &= \boldsymbol{G}_m(t), \end{aligned}$$

where $\tilde{\boldsymbol{R}}_m$ is the vector of degrees of freedom of $\boldsymbol{r}_m$ with respect to the basis $\{\tilde{\boldsymbol{v}}_i\}_{i=1}^m$;

$$(\tilde{\boldsymbol{A}}_m)_{ij} = (\boldsymbol{D}^{-1}\tilde{\boldsymbol{v}}_j,\tilde{\boldsymbol{v}}_i) + (\breve{\alpha}\tilde{\boldsymbol{v}}_j\cdot\boldsymbol{n},\tilde{\boldsymbol{v}}_i\cdot\boldsymbol{n})_{\partial\Omega}, \qquad \forall 1 \le i,j \le m,$$

is symmetric and positive-definite,

$$(\tilde{\boldsymbol{B}}_{nm})_{ij} = (\nabla \cdot \tilde{\boldsymbol{v}}_j, \mu_i) \text{ and } (\boldsymbol{G}_m(t))_i = (-\breve{\alpha} g(t), \tilde{\boldsymbol{v}}_i \cdot \boldsymbol{n})_{\partial\Omega}, \quad \forall\, 1 \le i \le n, 1 \le j \le m.$$

Thus, there exists a unique solution $(c_n, \boldsymbol{r}_m)$ to (3.3).

Now to prove the existence of a solution to (3.2), we derive suitable energy estimates in the same manner as in Section 2 but with an extra term $\boldsymbol{r}\cdot\boldsymbol{n}$ on the boundary.

LEMMA 3.2. *Let* $f \in L^2(0,T;L^2(\Omega))$, $g \in H^1(0,T;L^2(\partial\Omega)$ *and* $c_0 \in H^1(\Omega)$. *The following estimates hold*

$$\begin{aligned} &(i)\ \|c\|_{L^\infty(0,T;L^2(\Omega))} + \|\boldsymbol{r}\|_{L^2(0,T;\boldsymbol{L^2(\Omega)})} + \|\boldsymbol{r}\cdot\boldsymbol{n}\|_{L^2(0,T;L^2(\partial\Omega))} \\ &\qquad \le C(\|c_0\|_{L^2(\Omega)} + \|f\|_{L^2(0,T;L^2(\Omega))} + \|g\|_{L^2(0,T;L^2(\partial\Omega))}), \\ &(ii)\ \|\partial_t c\|_{L^2(0,T;L^2(\Omega))} + \|\boldsymbol{r}\|_{L^\infty(0,T;\boldsymbol{L^2(\Omega)})} + \|\boldsymbol{r}\cdot\boldsymbol{n}\|_{L^\infty(0,T;L^2(\partial\Omega))} \\ &\qquad \le C(\|c_0\|_{H^1(\Omega)} + \|f\|_{L^2(0,T;L^2(\Omega))} + \|g\|_{H^1(0,T;L^2(\partial\Omega))}), \\ &(iii)\ \|\boldsymbol{r}\|_{L^2(0,T;\mathcal{H}(div,\Omega))} \le C(\|c_0\|_{H^1(\Omega)} + \|f\|_{L^2(0,T;L^2(\Omega))} + \|g\|_{H^1(0,T;L^2(\partial\Omega))}). \end{aligned}$$

LEMMA 3.3. (Estimates with greater regularity) *Assume that* $\boldsymbol{D}$ *is in* $\boldsymbol{W^{1,\infty}(\Omega)}$, c_0 *in* $H^2(\Omega)$, f *in* $H^1(0,T;L^2(\Omega))$ *and* g *in* $H^1(0,T;L^2(\partial\Omega))$, *then*

$$\begin{aligned} &\|\partial_t c\|_{L^\infty(0,T;L^2(\Omega))} + \|\boldsymbol{r}\|_{L^\infty(0,T;\mathcal{H}(\mathrm{div},\Omega))} + \|\partial_t \boldsymbol{r}\|_{L^2(0,T;\boldsymbol{L^2(\Omega)})} \\ &\qquad \le C(\|f\|_{H^1(0,T;L^2(\Omega))} + \|c_0\|_{H^2(\Omega)} + \|g\|_{H^1(0,T;L^2(\partial\Omega))}). \end{aligned}$$

Proof. (of Lemma 3.2). In order to prove *(i)*, as before, we take c_n and $\boldsymbol{r}_m$ as test functions in (3.3) and add the two equations:

$$(\omega\partial_t c_n, c_n) + \big(\boldsymbol{D}^{-1}\boldsymbol{r}_m, \boldsymbol{r}_m\big) + (\breve{\alpha}\boldsymbol{r}_m\cdot\boldsymbol{n}, \boldsymbol{r}_m\cdot\boldsymbol{n})_{\partial\Omega} = (f, c_n) + (-\breve{\alpha} g, \boldsymbol{r}_m\cdot\boldsymbol{n})_{\partial\Omega}\,.$$

The assumptions concerning ω, $\boldsymbol{D}$ and $\breve{\alpha}$ give

$$(\omega\partial_t c_n, c_n) \ge \frac{\omega_-}{2}\frac{d}{dt}\|c_n\|^2,\ \ (\boldsymbol{D}^{-1}\boldsymbol{r}_m, \boldsymbol{r}_m) \ge \delta_-\|\boldsymbol{r}_m\|^2,\ \ (\breve{\alpha}\boldsymbol{r}_m\cdot\boldsymbol{n}, \boldsymbol{r}_m\cdot\boldsymbol{n})_{\partial\Omega} \ge \kappa_1\|\boldsymbol{r}_m\cdot\boldsymbol{n}\|^2_{\partial\Omega},$$

and the Cauchy-Schwarz inequality:

$$|\ (f, c_n)\ | \le \|f\|\|c_n\| \le \frac{1}{2\omega_-}\|f\|^2 + \frac{\omega_-}{2}\|c_n\|^2. \tag{3.4}$$

Similarly, for each $\epsilon > 0$,

$$|-(\breve{\alpha} g, \boldsymbol{r}_m\cdot\boldsymbol{n})_{\partial\Omega}\ | \le \kappa_2\|g\|_{\partial\Omega}\ \|\boldsymbol{r}_m\cdot\boldsymbol{n}\|_{\partial\Omega} \le \kappa_2\left(\frac{1}{2\epsilon}\|g\|^2_{\partial\Omega} + \frac{\epsilon}{2}\|\boldsymbol{r}_m\cdot\boldsymbol{n}\|^2_{\partial\Omega}\right). \tag{3.5}$$

Choosing $\epsilon = \dfrac{\kappa_1}{\kappa_2}$, we then obtain

$$\frac{\omega_-}{2}\frac{d}{dt}\|c_n\|^2 + \delta_-\|\boldsymbol{r}_m\|^2 + \frac{\kappa_1}{2}\|\boldsymbol{r}_m\cdot\boldsymbol{n}\|^2_{\partial\Omega} \le \frac{1}{2\omega_-}\|f\|^2 + \frac{\kappa_2^2}{2\kappa_1}\|g\|^2_{\partial\Omega} + \frac{\omega_-}{2}\|c_n\|^2.$$

Integrating this inequality over $(0,t)$ for $t \in (0,T]$, and using $\|c_n(0)\|^2 \le \|c_0\|^2$, we get

$$\|c_n(t)\|^2 + \frac{2\delta_-}{\omega_-}\int_0^t \|\boldsymbol{r}_m(s)\|^2\,ds + \frac{\kappa_1}{\omega_-}\int_0^t \|\boldsymbol{r}_m(s)\cdot\boldsymbol{n}\|_{\partial\Omega}^2\,ds$$
$$\le C\left(\|c_0\|^2 + \|f\|^2_{L^2(0,T;L^2(\Omega))} + \|g\|^2_{L^2(0,T;L^2(\partial\Omega))}\right) + \int_0^t \|c_n(s)\|^2\,ds,$$

with $C = \max(1, \dfrac{1}{\omega_-^2}, \dfrac{\kappa_2^2}{\omega_-\kappa_1})$. Then an application of Gronwall's lemma completes the proof of (i).

For *(ii)*, we follow the same steps as in (2.12)-(2.15): taking $\partial_t c_n \in L^2(0,T;M)$ as the test function in the first equation of (3.3), we obtain

$$(\omega\partial_t c, \partial_t c) + (\nabla\cdot\boldsymbol{r}_m, \partial_t c) = (f, \partial_t c). \tag{3.6}$$

Differentiating the second equation of (3.3) with respect to t, we obtain

$$-(\nabla\cdot\boldsymbol{v}, \partial_t c_n) + (\boldsymbol{D}^{-1}\partial_t\boldsymbol{r}_m, \boldsymbol{v}) + (\breve{\alpha}\partial_t\boldsymbol{r}_m\cdot\boldsymbol{n}, \boldsymbol{v}\cdot\boldsymbol{n})_{\partial\Omega} = -(\breve{\alpha}\partial_t g, \boldsymbol{v}\cdot\boldsymbol{n})_{\partial\Omega},\ \forall\boldsymbol{v}\in\widetilde{\Sigma}.$$

Then we take $\boldsymbol{v} = \boldsymbol{r}_m$ in the previous equation and add the resulting equation to (3.6) to obtain

$$(\omega\partial_t c_n, \partial_t c_n) + (\boldsymbol{D}^{-1}\partial_t\boldsymbol{r}_m, \boldsymbol{r}_m) + (\breve{\alpha}\partial_t\boldsymbol{r}_m\cdot\boldsymbol{n}, \boldsymbol{r}_m\cdot\boldsymbol{n})_{\partial\Omega} = (f, \partial_t c_n) - (\breve{\alpha}\partial_t g, \boldsymbol{r}_m\cdot\boldsymbol{n})_{\partial\Omega}.$$

As $\boldsymbol{D}$ is symmetric and positive definite, by applying the Cauchy-Schwarz inequality to the right hand side as well as using the property of ω, we obtain

$$\omega_-\|\partial_t c\|^2 + \frac{1}{2}\frac{d}{dt}\|\sqrt{\boldsymbol{D}^{-1}}\boldsymbol{r}_m\|^2 + \frac{\kappa_1}{2}\frac{d}{dt}\|\boldsymbol{r}_m\cdot\boldsymbol{n}\|^2_{\partial\Omega} \le |\,(f,\partial_t c)\,| + |\,(\breve{\alpha}\partial_t g, \boldsymbol{r}_m\cdot\boldsymbol{n})_{\partial\Omega}\,|.$$

We then apply the Cauchy-Schwarz inequality for the right-hand side (as in (3.4), (3.5), replacing c and g by $\partial_t c$ and $\partial_t g$), and take $\epsilon = \dfrac{\kappa_1}{\kappa_2}$, $C = \max(\dfrac{1}{\omega_-}, \dfrac{\kappa_2^2}{\kappa_1})$ to obtain

$$\omega_-\|\partial_t c_n\|^2 + \frac{d}{dt}\|\sqrt{\boldsymbol{D}^{-1}}\boldsymbol{r}_m\|^2 + \kappa_1\frac{d}{dt}\|\boldsymbol{r}_m\cdot\boldsymbol{n}\|^2_{\partial\Omega} \le C\left(\|f\|^2 + \|\partial_t g\|^2_{\partial\Omega}\right) + \kappa_1\|\boldsymbol{r}_m\cdot\boldsymbol{n}\|^2_{\partial\Omega}.$$

Integrating over $(0,t)$ for $t\in[0,T]$, we find

$$\omega_-\int_0^t \|\partial_t c_n(s)\|^2 ds + \|\sqrt{\boldsymbol{D}^{-1}}\boldsymbol{r}_m(t)\|^2 + \kappa_1\|\boldsymbol{r}_m(t)\cdot\boldsymbol{n}\|^2_{\partial\Omega}$$
$$\le C(\|f\|^2_{L^2(0,T;L^2(\Omega))} + \|g\|^2_{H^1(0,T;L^2(\partial\Omega))}) + \|\sqrt{\boldsymbol{D}^{-1}}\boldsymbol{r}_m(0)\|^2 + \kappa_1\|\boldsymbol{r}_m(0)\cdot\boldsymbol{n}\|^2_{\partial\Omega}$$
$$+\kappa_1\int_0^t \|\boldsymbol{r}_m(s)\cdot\boldsymbol{n}\|^2_{\partial\Omega}ds. \tag{3.7}$$

So there only remains to bound the term $(\|\sqrt{\boldsymbol{D}^{-1}}\boldsymbol{r}_m(0)\|^2 + \kappa_1\|\boldsymbol{r}_m(0)\cdot\boldsymbol{n}\|^2_{\partial\Omega})$. Toward this end, we use the second equation of (3.3) with $\boldsymbol{v} = \boldsymbol{r}_m$ and for $t=0$ to obtain:

$$\delta_-\|\boldsymbol{r}_m(0)\|^2 + \kappa_1\|\boldsymbol{r}_m(0)\cdot\boldsymbol{n}\|^2 \le (\nabla\cdot\boldsymbol{r}_m(0), c_n(0)) + (-\breve{\alpha}g(0), \boldsymbol{r}_m(0)\cdot\boldsymbol{n})_{\partial\Omega}.$$

Let $n \to \infty$, as $c_n(0) \to c_0$ we have

$$\begin{aligned}\delta_- \|\boldsymbol{r}_m(0)\|^2 + \kappa_1 \|\boldsymbol{r}_m(0)\cdot\boldsymbol{n}\|^2 &\le (\nabla\cdot\boldsymbol{r}_m(0), c_0) + (-\breve{\alpha} g(0), \boldsymbol{r}_m(0)\cdot\boldsymbol{n})_{\partial\Omega}\\ &\le (-\boldsymbol{r}_m(0), \nabla c_0) + (c_0 - \breve{\alpha} g(0), \boldsymbol{r}_m(0)\cdot\boldsymbol{n})_{\partial\Omega}\\ &\le \frac{\delta_-}{2}\|\boldsymbol{r}_m(0)\|^2 + \frac{1}{2\delta_-}\|\nabla c_0\|^2 + \frac{\kappa_1}{2}\|\boldsymbol{r}_m(0)\cdot\boldsymbol{n}\|^2 + \frac{\kappa_2}{2\kappa_1}\|c_0 - g(0)\|^2_{\partial\Omega},\end{aligned}$$

or

$$\delta_- \|\boldsymbol{r}_m(0)\|^2 + \kappa_1 \|\boldsymbol{r}_m(0)\cdot\boldsymbol{n}\|^2 \le C\left(\|c_0\|^2_{H^1(\Omega)} + \|g\|^2_{H^1(0,T;L^2(\partial\Omega))}\right).$$

This along with (3.7) and Gronwall's lemma yields (ii). We now estimate $\|\nabla\cdot\boldsymbol{r}_m\|^2$ as in Section 2: we derive (2.21) from (2.20) and the first equation of (3.3) (after multiplying by $\xi^i_m(t)$ and summing over $i = 1, \dots, n$). Then, using the bound for $\|\partial_t c\|_{L^2(0,T;L^2(\Omega))}$ in (ii), we obtain

$$\|\nabla\cdot\boldsymbol{r}_m\|^2_{L^2(0,T;L^2(\Omega))} \le C(\|c_0\|^2_{H^1(\Omega)} + \|f\|^2_{L^2(0,T;L^2(\Omega))} + \|g\|^2_{H^1(0,T;L^2(\partial\Omega))}). \quad (3.8)$$

This along with (i) gives

$$\|\boldsymbol{r}_m\|^2_{L^2(0,T;\mathcal{H}(\mathrm{div},\Omega))} \le C(\|c_0\|^2_{H^1(\Omega)} + \|f\|^2_{L^2(0,T;L^2(\Omega))} + \|g\|^2_{H^1(0,T;L^2(\partial\Omega))}),$$

and the proof of Lemma 3.2 is completed. $\square$

We now prove Lemma 3.3 for the higher regularity of the solution to (2.3).

Proof. (of Lemma 3.3). Let $n, m \ge 1$. Differentiate both equations of (3.3) with respect to t, take $\mu = \partial_t c_n$ and $\boldsymbol{v} = \partial_t \boldsymbol{r}_m$ as the test functions, and add the two resulting equations to obtain

$$\begin{aligned}(\omega\partial_{tt}c_n, \partial_t c_n) + (\boldsymbol{D}^{-1}\partial_t\boldsymbol{r}_m, \partial_t\boldsymbol{r}_m) + (\breve{\alpha}\partial_t\boldsymbol{r}_m\cdot\boldsymbol{n}, \partial_t\boldsymbol{r}_m\cdot\boldsymbol{n})_{\partial\Omega}&\\ = (\partial_t f, \partial_t c_n) - (\breve{\alpha}\partial_t g, \partial_t\boldsymbol{r}_m\cdot\boldsymbol{n})_{\partial\Omega}&.\end{aligned}$$

Then, the assumptions concerning ω, $\boldsymbol{D}$, $\breve{\alpha}$, and the Cauchy-Schwarz inequality give

$$\frac{\omega_-}{2}\frac{d}{dt}\|\partial_t c_n\|^2 + \delta_-\|\partial_t\boldsymbol{r}_m\|^2 + \frac{\kappa_1}{2}\|\partial_t\boldsymbol{r}_m\cdot\boldsymbol{n}\|^2_{\partial\Omega} \le \frac{1}{2\omega_-}\|\partial_t f\|^2 + \frac{\kappa_2^2}{2\kappa_1}\|\partial_t g\|^2_{\partial\Omega} + \frac{\omega_-}{2}\|\partial_t c_n\|^2.$$

Integrating this inequality over $(0, t)$, for for $t \in (0, T]$, we obtain

$$\begin{aligned}&\|\partial_t c_n(t)\|^2 + \frac{2\delta_-}{\omega_-}\int_0^t \|\partial_t\boldsymbol{r}_m(s)\|^2\,ds + \frac{\kappa_1}{\omega_-}\int_0^t \|\partial_t\boldsymbol{r}_m(s)\cdot\boldsymbol{n}\|^2_{\partial\Omega}\,ds\\ &\le C(\|\partial_t c_n(0)\|^2 + \|\partial_t f\|^2_{L^2(0,T;L^2(\Omega))} + \|\partial_t g\|^2_{L^2(0,T;L^2(\partial\Omega))}) + \int_0^t \|\partial_t c_n(s)\|^2\,ds, \quad (3.9)\end{aligned}$$

with $C = \max(1, \frac{1}{\omega_-^2}, \frac{\kappa_2^2}{\omega_-\kappa_1})$. To bound $\|\partial_t c_n(0)\|$, we use the first equation of (3.3) at $t = 0$ with $\mu = \partial_t c_n$, and the Cauchy-Schwarz inequality to obtain

$$\|\partial_t c_n(0)\|^2 \le C(\|f(0)\|^2 + \|\nabla\cdot\boldsymbol{r}_m(0)\|^2) \le C(\|f(0)\|^2 + \|c_0\|^2_{H^2(\Omega)}).$$

Here we have used the fact that $\boldsymbol{D}^{-1}\boldsymbol{r}_m(0) = -\nabla c_n(0)$ in $\mathcal{D}'(\Omega)$ given by the second equation of (3.3), and hence in $L^2(\Omega)$ since $c_0 \in H^2(\Omega)$. From this inequality and

(3.9), we have

$$\|\partial_t c_n(t)\|^2 + \frac{2\delta_-}{\omega_-}\int_0^t \|\partial_t \boldsymbol{r}_m(s)\|^2\,ds + \frac{\kappa_1}{\omega_-}\int_0^t \|\partial_t \boldsymbol{r}_m(s)\cdot \boldsymbol{n}\|^2_{\partial\Omega}\,ds$$
$$\leq C(\|c_0\|^2_{H^2(\Omega)} + \|f\|^2_{H^1(0,T;L^2(\Omega))} + \|g\|^2_{H^1(0,T;L^2(\partial\Omega))}) + \int_0^t \|\partial_t c_n\|^2 ds. \quad (3.10)$$

It now follows from (3.10) and Gronwall's lemma that

$$\|\partial_t c_n\|_{L^\infty(0,T;L^2(\Omega))} + \|\partial_t \boldsymbol{r}_m\|_{L^2(0,T;\boldsymbol{L^2(\Omega)})} + \|\partial_t \boldsymbol{r}_m\cdot \boldsymbol{n}\|_{L^2(0,T;L^2(\partial\Omega))}$$
$$\leq C(\|c_0\|^2_{H^2(\Omega)} + \|f\|^2_{H^1(0,T;L^2(\Omega))} + \|g\|^2_{H^1(0,T;L^2(\partial\Omega))}). \quad (3.11)$$

To obtain the estimate in the $\mathcal{H}(\mathrm{div},\Omega)$-norm, we follow the same steps as for (3.8) to obtain

$$\|\nabla\cdot \boldsymbol{r}_m\|^2_{L^\infty(0,T;L^2(\Omega))} \leq C(\|c_0\|^2_{H^2(\Omega)} + \|f\|^2_{H^1(0,T;L^2(\Omega))} + \|g\|^2_{H^1(0,T;L^2(\partial\Omega))}).$$

This along with the inequality (i) of Lemma 3.2 gives

$$\|\boldsymbol{r}\|^2_{L^\infty(0,T;\mathcal{H}(\mathrm{div},\Omega))} \leq C(\|c_0\|^2_{H^2(\Omega)} + \|f\|^2_{H^1(0,T;L^2(\Omega))} + \|g\|^2_{H^1(0,T;L^2(\partial\Omega))}). \quad (3.12)$$

The lemma now follows from (3.11) and (3.12). ◻

Thanks to Lemma 3.2, we can finish the proof of Theorem 3.1 using similar arguments as for the proof of Theorem 2.1. ◻

4. Space-time domain decomposition methods. In this section, we present two nonoverlapping domain decomposition methods for solving problem (2.3). For simplicity, we consider a decomposition of Ω into two non overlapping subdomains Ω_1 and Ω_2 separated by an interface Γ:

$$\Omega_1 \cap \Omega_2 = \emptyset; \quad \Gamma = \partial\Omega_1 \cap \partial\Omega_2 \cap \Omega, \quad \Omega = \Omega_1 \cup \Omega_2 \cup \Gamma.$$

Also for the sake of simplicity we have assumed throughout this section and the next that the boundary condition given on $\partial\Omega$ is a homogeneous Dirichlet condition. However, the analysis given below can be generalized to the case of multiple subdomains and more general boundary conditions (see Section 6).

For $i = 1, 2$, let $\boldsymbol{n}_i$ denote the unit outward pointing vector field on $\partial\Omega_i$, and for any scalar, vector or tensor valued function φ defined on Ω, let φ_i denote the restriction of φ to Ω_i. Using this notation, problem (2.3) can be reformulated as an equivalent multidomain problem consisting of the following space-time subdomain problems

$$\left.\begin{array}{rll} \omega_i\partial_t c_i + \nabla\cdot \boldsymbol{r}_i &= f & \text{in } \Omega_i\times(0,T),\\ \nabla c_i + \boldsymbol{D}_i^{-1}\boldsymbol{r}_i &= 0 & \text{in } \Omega_i\times(0,T),\\ c_i &= 0 & \text{on } \partial\Omega_i\cap\partial\Omega\times(0,T),\\ c_i(0) &= c_0 & \text{in } \Omega_i, \end{array}\right. \quad \text{for } i=1,2, \quad (4.1)$$

together with the transmission conditions on the space-time interface

$$\begin{array}{l} c_1 = c_2 \\ \boldsymbol{r}_1\cdot\boldsymbol{n}_1 + \boldsymbol{r}_2\cdot\boldsymbol{n}_2 = 0 \end{array} \qquad \text{on } \Gamma\times(0,T), \quad (4.2)$$

Alternatively, and equivalently, one may impose the transmission conditions

$$\begin{aligned} -\boldsymbol{r}_1\cdot\boldsymbol{n}_1+\alpha_{1,2}c_1 &= -\boldsymbol{r}_2\cdot\boldsymbol{n}_1+\alpha_{1,2}c_2 \\ -\boldsymbol{r}_2\cdot\boldsymbol{n}_2+\alpha_{2,1}c_2 &= -\boldsymbol{r}_1\cdot\boldsymbol{n}_2+\alpha_{2,1}c_1 \end{aligned} \quad \text{on } \Gamma\times(0,T)\,, \tag{4.3}$$

where $\alpha_{1,2}$ and $\alpha_{2,1}$ are a pair of positive parameters. The first method that we consider is based on (4.1) together with the "natural" transmission conditions (4.2) while the second method is based on (4.1) together with the Robin transmission conditions (4.3). For the latter method the parameters $\alpha_{i,j}$ may be optimized to improve the convergence rate of the iterative scheme (see [1, 10, 11, 12]).

For both methods the multidomain problem is formulated through the use of interface operators as a problem posed on the space-time interface. For the first method the interface operators are time-dependent Steklov-Poincaré (Dirichlet-to-Neumann) operators while for the second they are Robin-to-Robin operators. Associated with a Jacobi algorithm this latter method is known as the Optimized Schwarz Waveform Relaxation (OSWR) method. Rewriting the OSWR method as a space-time interface problem solved by a more general (Krylov) method was done in [14]; here we extend that work to a problem written in mixed form.

4.1. Method 1: Using the time-dependent Steklov-Poincaré operator. To introduce the interface problem for this method we introduce several operators, but first we define some notation:

$$\Lambda = H^1(0,T;H^{\frac12}_{00}(\Gamma)), \quad \text{and, for } i=1,2, \quad M_i = L^2(\Omega_i) \quad \text{and} \quad \Sigma_i = H(\mathrm{div},\Omega_i).$$

We also define $H^1_*(\Omega_i)=\{v\in H^1(\Omega_i),\ v=0 \text{ over } \partial\Omega_i\cap\partial\Omega\}$, for $i=1,2$.
Next, let $\mathcal{D}_i, i=1,2$, be the solution operator that associates to the boundary, right-hand-side, and initial data (λ, f, c_0) the solution $(c_i,\boldsymbol{r}_i)$ of the subdomain problem

$$\begin{aligned} \omega_i\partial_t c_i+\nabla\cdot\boldsymbol{r}_i &= f && \text{in } \Omega_i\times(0,T)\,,\\ \nabla c_i+\boldsymbol{D}_i^{-1}\boldsymbol{r}_i &= 0 && \text{in } \Omega_i\times(0,T)\,,\\ c_i &= 0 && \text{on } \partial\Omega_i\cap\partial\Omega\times(0,T),\\ c_i &= \lambda && \text{on } \Gamma\times(0,T)\,,\\ c_i(0) &= c_0 && \text{in } \Omega_i. \end{aligned} \tag{4.4}$$

An extension of Theorem 2.1 (to the case of non-homogeneous Dirichlet boundary conditions) guarantees that

$$\begin{aligned} \mathcal{D}_i\ :\ \ \Lambda\times L^2(0,T;L^2(\Omega_i))\times H^1_*(\Omega_i) &\longrightarrow H^1(0,T;M_i)\times L^2(0,T;\Sigma_i)\\ (\lambda,f,c_0) &\mapsto (c_i,\boldsymbol{r}_i)=(c_i(\lambda,f,c_0),\boldsymbol{r}_i(\lambda,f,c_0)) \end{aligned}$$

is a well defined operator. We also make use of the normal trace operator

$$\begin{aligned} \mathcal{F}_i\ :\ \ H^1(0,T;M_i))\times L^2(0,T;\Sigma_i) &\longrightarrow L^2(0,T;(H^{\frac12}_{00}(\Gamma))')\\ (c_i,\boldsymbol{r}_i) &\mapsto \boldsymbol{r}_i\cdot\boldsymbol{n}_i|_{\Gamma\times(0,T)} \end{aligned}$$

which is then used to define the following operators:

$$\begin{aligned} \mathcal{S}_i\ :\ \ \Lambda &\longrightarrow L^2(0,T;(H^{\frac12}_{00}(\Gamma))')\\ \lambda &\mapsto -\mathcal{F}_i\mathcal{D}_i(\lambda,0,0) \end{aligned}$$

and

$$\begin{aligned} \chi_i\ :\ \ L^2(0,T;L^2(\Omega_i))\times H^1_*(\Omega_i) &\longrightarrow L^2(0,T;(H^{\frac12}_{00}(\Gamma))')\\ (f,c_0) &\mapsto \mathcal{F}_i\mathcal{D}_i(0,f,c_0). \end{aligned}$$

Now letting $\mathcal{S} = \mathcal{S}_1 + \mathcal{S}_2$ and $\chi = \chi_1 + \chi_2$ we may rewrite problem (4.1), (4.2) as the interface problem

$$\mathcal{S}\lambda = \chi(f, c_0), \qquad \text{on } \Gamma \times (0,T)\,. \tag{4.5}$$

The weak formulation of this problem is then

Find $\lambda \in \Lambda$ such that:

$$\int_0^T \langle \mathcal{S}\lambda, \eta\rangle = \int_0^T \langle \chi(f, c_0), \eta\rangle, \quad \forall \eta \in \Lambda, \tag{4.6}$$

where $\langle \cdot, \cdot\rangle$ denotes the duality pairing between $H_{00}^{\frac{1}{2}}(\Gamma)$ and $(H_{00}^{\frac{1}{2}}(\Gamma))'$. The operator $\mathcal{S}$ is the time-dependent Steklov-Poincaré operator, and to investigate its properties we write the weak formulation of the interface problem (4.4) for $f = 0$ and $c_0 = 0$:

For a.e. $t \in (0,T)$, find $c_i(t) \in M_i$ and $\boldsymbol{r}_i(t) \in \Sigma_i$ such that

$$\begin{aligned} \frac{d}{dt}(\omega_i c_i, \mu)_{\Omega_i} + (\nabla \cdot \boldsymbol{r}_i, \mu)_{\Omega_i} &= 0, && \forall \mu \in M_i, \\ -(\nabla \cdot \boldsymbol{v}, c_i)_{\Omega_i} + (\boldsymbol{D}_i^{-1}\boldsymbol{r}_i, \boldsymbol{v})_{\Omega_i} &= -\int_\Gamma \lambda(\boldsymbol{v}\cdot \boldsymbol{n}_i), && \forall \boldsymbol{v} \in \Sigma_i. \end{aligned} \tag{4.7}$$

For $\lambda \in \Lambda$ and for $i = 1, 2$, we will denote by $(c_i(\lambda), \boldsymbol{r}_i(\lambda))$ the solution of (4.7) for the data function λ. Then for $\eta, \lambda \in \Lambda$ and for almost every $t \in (0,T)$, we have

$$\begin{aligned} (\omega_i \partial_t c_i(\lambda), c_i(\eta))_{\Omega_i} + (\nabla \cdot \boldsymbol{r}_i(\lambda), c_i(\eta))_{\Omega_i} &= 0, \\ -(\nabla \cdot \boldsymbol{r}_i(\eta), c_i(\lambda))_{\Omega_i} + (\boldsymbol{D}_i^{-1}\boldsymbol{r}_i(\lambda), \boldsymbol{r}_i(\eta))_{\Omega_i} &= -\int_\Gamma \lambda(\boldsymbol{r}_i(\eta)\cdot \boldsymbol{n}_i). \end{aligned}$$

Now adding the first equation to the second equation in which the roles of λ and η are reversed, integrating over time and summing on i, we obtain

$$\sum_{i=1}^2 \int_0^T \left((\omega_i \partial_t c_i(\lambda), c_i(\eta))_{\Omega_i} + (\boldsymbol{D}_i^{-1}\boldsymbol{r}_i(\eta), \boldsymbol{r}_i(\lambda))_{\Omega_i}\right) \quad = -\sum_{i=1}^2 \int_0^T \int_\Gamma \eta(\boldsymbol{r}_i(\lambda)\cdot \boldsymbol{n}_i).$$

Thus we see that

$$\int_0^T \langle \mathcal{S}\lambda, \eta\rangle = -\sum_{i=1}^2 \int_0^T \int_\Gamma (\boldsymbol{r}_i(\lambda)\cdot \boldsymbol{n}_i)\eta = \sum_{i=1}^2 \int_0^T \left((\omega_i \partial_t c_i(\lambda), c_i(\eta))_{\Omega_i} + (\boldsymbol{D}_i^{-1}\boldsymbol{r}_i(\lambda), \boldsymbol{r}_i(\eta))_{\Omega_i}\right),$$

from which we conclude that $\mathcal{S}$ is a positive definite but non-symmetric, space-time interface operator. Thus the existence and uniqueness of the solution of the space-time interface problem (4.6) does not follow in a standard way, and we have not pursued this question here.

Nonetheless, we solve a discretized version of problem (4.5) iteratively by using a Krylov method (e.g. GMRES). Once the discrete approximation to λ is obtained, we can construct the multi-domain solution of the discretized problem. Following the work in [22, 25] for elliptic problems with strong heterogeneities, we apply a Neumann-Neumann type preconditioner enhanced with averaging weights:

$$\left(\sigma_1 \mathcal{S}_1^{-1} + \sigma_2 \mathcal{S}_2^{-1}\right) \mathcal{S}\lambda = \tilde{\chi}, \tag{4.8}$$

where $\sigma_i : \Gamma \times (0,T) \to [0,1]$ is such that $\sigma_1 + \sigma_2 = 1$, and $\mathcal{S}_i^{-1}$, the Neumann-to-Dirichlet operator, is the (pseudo)-inverse of $\mathcal{S}_i$, for $i = 1, 2$.

4.2. Method 2: Using Optimized Schwarz Waveform Relaxation (OSWR). The function spaces that are needed to give the interface formulation of method 2 are

$$\Xi := H^1(0,T;L^2(\Gamma)), \quad \text{and, for } i=1,2, \quad M_i = L^2(\Omega_i) \quad \text{and} \quad \widetilde{\Sigma}_i = \mathcal{H}(\mathrm{div},\Omega_i).$$

To define the Robin-to-Robin operator we first define for $i=1,2$, the following solution operator $\mathcal{R}_i$ which depends on the parameter $\alpha_{i,j};\ j=3-i$:

$$\begin{array}{rccc} \mathcal{R}_i: & \Xi \times L^2(0,T;L^2(\Omega_i)) \times H^1_*(\Omega_i) & \longrightarrow & \Xi \times H^1(0,T;M_i) \times L^2(0,T;\widetilde{\Sigma}_i) \\ & (\xi,f,c_0) & \mapsto & (\xi,c_i,\boldsymbol{r}_i) = (\xi, c_i(\xi,f,c_0), \boldsymbol{r}_i(\xi,f,c_0)) \end{array}$$

where $(c_i,\boldsymbol{r}_i) = (c_i(\xi,f,c_0),\boldsymbol{r}_i(\xi,f,c_0))$ is the solution to the problem

$$\begin{aligned} \omega_i\partial_t c_i + \nabla\cdot\boldsymbol{r}_i &= f && \text{in } \Omega_i\times(0,T)\,, \\ \nabla c_i + \boldsymbol{D}_i^{-1}\boldsymbol{r}_i &= 0 && \text{in } \Omega_i\times(0,T)\,, \\ c_i &= 0 && \text{on } \partial\Omega_i\cap\partial\Omega\times(0,T), \\ -\boldsymbol{r}_i\cdot\boldsymbol{n}_i + \alpha_{i,j}c_i &= \xi && \text{on } \Gamma\times(0,T)\,, \\ c_i(0) &= c_0 && \text{in } \Omega_i. \end{aligned} \tag{4.9}$$

(As stated earlier the parameters $\alpha_{i,j}$ will be chosen is such a way as to optimize the convergence of the algorithm). The existence and uniqueness of the solution of problem (4.9) is guaranteed by Theorem 3.1.
Next, to impose the interface conditions (4.3) we will need the following interface operators defined for $i=1,2$, and $j=3-i$:

$$\begin{array}{rccc} \mathcal{B}_i: & \left(\Xi\times H^1(0,T;M_j)\times L^2(0,T;\widetilde{\Sigma}_j)\right)\cap \mathrm{Im}(\mathcal{R}_j) & \longrightarrow & \Xi \\ & (\xi,c_j,\boldsymbol{r}_j) & \mapsto & (-\boldsymbol{r}_j\cdot\boldsymbol{n}_i + \dfrac{\alpha_{i,j}}{\alpha_{j,i}}(\xi+\boldsymbol{r}_j\cdot\boldsymbol{n}_j))|_{\Gamma\times(0,T)} \end{array}$$

Remark 4.1. *To see that $Im(\mathcal{B}_i)\subset\Xi$ (instead of simply $L^2(0,T;L^2(\Gamma))$, we note that* (3.2) *implies that $\boldsymbol{D}^{-1}\boldsymbol{r}(t) = -\nabla c(t)$ in $\mathcal{D}'(\Omega)$ for a.e. $t\in(0,T)$. Since $\boldsymbol{r}(t)$ is in $H(div,\Omega)$, we have $c(t)\in H^1(\Omega)$, for a.e. $t\in(0,T)$. Consequently, $c_i(t)$ is in $H^1(0,T;H^1(\Omega_i))$. This along with the fact that $\xi\in\Xi$ implies that $\boldsymbol{r}_i\cdot\boldsymbol{n}_i|_{\Gamma\times(0,T)}\in\Xi$.*

Now, defining

$$\begin{array}{rccc} \mathcal{S}_R: & \Xi\times\Xi & \longrightarrow & \Xi\times\Xi \\ & \begin{pmatrix}\xi_1\\ \xi_2\end{pmatrix} & \mapsto & \begin{pmatrix}\xi_1 - \mathcal{B}_1\mathcal{R}_2(\xi_2,0,0)\\ \xi_2 - \mathcal{B}_2\mathcal{R}_1(\xi_1,0,0)\end{pmatrix} \end{array}$$

and

$$\begin{array}{rccc} \chi_R: & L^2(0,T;L^2(\Omega_i))\times H^1_*(\Omega_i) & \longrightarrow & \Xi\times\Xi \\ & (f,c_0) & \mapsto & \begin{pmatrix}\mathcal{B}_1\mathcal{R}_2(0,f,c_0)\\ \mathcal{B}_2\mathcal{R}_1(0,f,c_0)\end{pmatrix}, \end{array}$$

we can write the interface problem as

$$\mathcal{S}_R\begin{pmatrix}\xi_1\\ \xi_2\end{pmatrix} = \chi_R(f,c_0) \quad \text{on } \Gamma\times(0,T). \tag{4.10}$$

We then write (4.10) in weak form as

Find $(\xi_1,\xi_2) \in \Xi \times \Xi$ such that

$$\int_0^T \int_\Gamma \mathcal{S}_R \begin{pmatrix}\xi_1\\ \xi_2\end{pmatrix} \cdot \begin{pmatrix}\zeta_1\\ \zeta_2\end{pmatrix} = \int_0^T \int_\Gamma \chi_R(f,c_0) \cdot \begin{pmatrix}\zeta_1\\ \zeta_2\end{pmatrix}, \quad \forall (\zeta_1,\zeta_2) \in \Xi \times \Xi. \tag{4.11}$$

In order to study the interface operator $\mathcal{S}_R$, we proceed as in the Section 4.1 by giving the weak formulation of the relevant subdomain problems (here (4.9) for $i = 1,2$ and $j = 3-1$) for $f = 0$ and $c_0 = 0$:

For a.e. $t \in (0,T)$, find $c_i(t) \in M_i$ and $\boldsymbol{r}_i(t) \in \widetilde{\Sigma}_i$ such that, $\forall \mu \in M_i$ and $\forall \boldsymbol{v} \in \widetilde{\Sigma}_i$,

$$\begin{aligned} \frac{d}{dt}(\omega_i c_i,\mu)_{\Omega_i} + (\nabla\cdot\boldsymbol{r}_i,\mu)_{\Omega_i} &= 0,\\ -(\nabla\cdot\boldsymbol{v},c_i)_{\Omega_i} + (\boldsymbol{D}_i^{-1}\boldsymbol{r}_i,\boldsymbol{v})_{\Omega_i} + \int_\Gamma \frac{1}{\alpha_{i,j}}(\boldsymbol{r}_i\cdot\boldsymbol{n}_i)(\boldsymbol{v}\cdot\boldsymbol{n}_i) &= -\int_\Gamma \frac{1}{\alpha_{i,j}}\xi(\boldsymbol{v}\cdot\boldsymbol{n}_i). \end{aligned} \tag{4.12}$$

Now for any $\zeta \in \Xi$ letting $c_i(\zeta) \in H^1(0,T;M_i)$ and $\boldsymbol{r}_i(\zeta) \in L^2(0,T;\widetilde{\Sigma}_i)$ be such that $\mathcal{R}_i(\zeta,0,0) = (\zeta, c_i(\zeta), \boldsymbol{r}_i(\zeta))$, we have for any pair of elements ξ and ζ in Ξ and for a.e. $t \in (0,T)$ that

$$\begin{aligned} &(\omega_i\partial_t c_i(\xi), c_i(\zeta))_{\Omega_i} + (\nabla\cdot\boldsymbol{r}_i(\xi), c_i(\zeta))_{\Omega_i} = 0,\\ &-(\nabla\cdot\boldsymbol{r}_i(\zeta), c_i(\xi))_{\Omega_i} + (\boldsymbol{D}_i^{-1}\boldsymbol{r}_i(\xi),\boldsymbol{r}_i(\zeta))_{\Omega_i} + \int_\Gamma \frac{1}{\alpha_{i,j}}(\boldsymbol{r}_i(\xi)\cdot\boldsymbol{n}_i)(\boldsymbol{r}_i(\zeta)\cdot\boldsymbol{n}_i)\\ &\qquad = -\int_\Gamma \frac{1}{\alpha_{i,j}}\xi(\boldsymbol{r}_i(\zeta)\cdot\boldsymbol{n}_i). \end{aligned}$$

Next we add the first of these two equations to the second in which the roles of ζ and ξ have been interchanged to obtain

$$\begin{aligned} (\omega_i\partial_t c_i(\xi), c_i(\zeta))_{\Omega_i} + (\boldsymbol{D}_i^{-1}\boldsymbol{r}_i(\xi),\boldsymbol{r}_i(\zeta))_{\Omega_i} + \int_\Gamma \frac{1}{\alpha_{i,j}}(\boldsymbol{r}_i(\xi)\cdot\boldsymbol{n}_i)(\boldsymbol{r}_i(\zeta)\cdot\boldsymbol{n}_i)&\\ = -\int_\Gamma \frac{1}{\alpha_{i,j}}\zeta(\boldsymbol{r}_i(\xi)\cdot\boldsymbol{n}_i),& \end{aligned} \tag{4.13}$$

and this holds for any pair of elements ξ and ζ in Ξ. Now we consider the case in which the parameters $\alpha_{i,j}$, $i = 1,2$, $j = 3-i$, are constant and apply (4.13) with $\xi = \xi_j$ and $\zeta = \zeta_i$, to obtain

$$\begin{aligned} \int_0^T \int_\Gamma \mathcal{S}_R \begin{pmatrix}\xi_1\\ \xi_2\end{pmatrix} \cdot \begin{pmatrix}\zeta_1\\ \zeta_2\end{pmatrix} = \sum_{i=1}^{2} \int_0^T \Big\{ \int_\Gamma (\xi_i - \frac{\alpha_{i,j}}{\alpha_{j,i}}\xi_j)\zeta_i + (\alpha_{1,2}+\alpha_{2,1})\Big\{(\omega_i\partial_t c_i(\xi_j), c_i(\zeta_i))_{\Omega_i}&\\ +(\boldsymbol{D}_i^{-1}\boldsymbol{r}_i(\xi_j),\boldsymbol{r}_i(\zeta_i))_{\Omega_i} + \int_\Gamma \frac{1}{\alpha_{i,j}}(\boldsymbol{r}_i(\xi_j)\cdot\boldsymbol{n}_i)(\boldsymbol{r}_i(\zeta_i)\cdot\boldsymbol{n}_i)\Big\}\Big\}& \end{aligned}$$

As for method 1, we obtain a non-symmetric, space-time interface operator, but here it is also not positive definite. We solve the discretized problem iteratively using Jacobi iterations or GMRES. The former choice is equivalent to the OSWR algorithm, and in the next subsection we show that this mixed form of the algorithm converges.

4.2.1. The OSWR algorithm. We consider the general case in which Ω is decomposed into I non-overlapping subdomains Ω_i. We denote by $\Gamma_{i,j}$ the interface between two neighboring subdomains Ω_i and Ω_j, $\Gamma_{i,j} = \partial\Omega_i \cap \partial\Omega_j \cap \Omega$. Let $\mathcal{N}_i$ be the set of indices of the neighbors of the subdomain Ω_i, $i = 1, \ldots, I$. The OSWR method may be written as follows: at the k^{th} iteration, we solve in each subdomain the problem

$$\begin{array}{lll} \partial_t c_i^k + \nabla \cdot \boldsymbol{r}_i^k & = f, & \text{in } \Omega_i \times (0,T), \\ \nabla c_i^k + \boldsymbol{D}_i^{-1} \boldsymbol{r}_i^k & = 0, & \text{in } \Omega_i \times (0,T), \\ -\boldsymbol{r}_i^k \cdot \boldsymbol{n}_i + \alpha_{i,j} c_i^k & = -\boldsymbol{r}_j^{k-1} \cdot \boldsymbol{n}_i + \alpha_{i,j} c_j^{k-1}, & \text{on } \Gamma_{i,j} \times (0,T), \forall j \in \mathcal{N}_i, \end{array} \tag{4.14}$$

where, for $i = 1, \cdots, I$, $j \in \mathcal{N}_i$, $\alpha_{i,j} > 0$ is a Robin parameter. The initial value is that of c_0 in each subdomain. Moreover, $(g_{i,j}) := -\boldsymbol{r}_j^0 \cdot \boldsymbol{n}_i + \alpha_{i,j} c_j^0$ is an initial guess on $\Gamma_{i,j}$, for $i = 1, \cdots, I$, $j \in \mathcal{N}_i$, in order to start the first iterate.

Theorem 4.2. *Let $\boldsymbol{D} \in \boldsymbol{W^{1,\infty}(\Omega)}$, $f \in H^1(0,T; L^2(\Omega))$ and $c_0 \in H^2(\Omega) \cap H_0^1(\Omega)$ and let $\alpha_{i,j} \in L^\infty(\partial\Omega_i)$ be such that $\alpha_{i,j} \geq \alpha_0 > 0$ for $i = 1, \cdots, I$, $j \in \mathcal{N}_i$. Algorithm (4.14), initialized by $(g_{i,j})$ in $H^1\left(0,T; L^2\left(\Gamma_{i,j}\right)\right)$, $i = 1, \cdots, I$, $j \in \mathcal{N}_i$, defines a sequence of iterates*

$$(c_i^k, \boldsymbol{r}_i^k) \in W^{1,\infty}(0,T; L^2(\Omega_i)) \times \left(L^2(0,T; \mathcal{H}(\mathrm{div}, \Omega_i)) \cap H^1(0,T; \boldsymbol{L^2(\Omega_i)})\right),$$

for $i = 1, \cdots, I$, that converges to the weak solution $(c, \boldsymbol{r})$ of problem (2.3).

Proof. The sequence $(c_i^k, \boldsymbol{r}_i^k)_k$ is well-defined according to Theorem 3.1 and Remark 4.1. Now, to prove the convergence of algorithm (4.14), as the equations are linear, we can take $f = 0$ and $c_0 = 0$ and show that the sequence $\left(c_i^k, \boldsymbol{r}_i^k\right)_k$ of iterates converges to zero in suitable norms.
To begin, we write the variational formulation of (4.14) (with $f = 0$):

For a.e. $t \in (0,T)$, find $c_i^k(t) \in M_i$ and $\boldsymbol{r}_i^k(t) \in \tilde{\Sigma}_i$ such that

$$\begin{array}{lll} \dfrac{d}{dt}(\omega c_i^k, \mu_i)_{\Omega_i} + (\nabla \cdot \boldsymbol{r}_i^k, \mu_i)_{\Omega_i} & = 0, & \forall \mu_i \in M_i, \\ -(\nabla \cdot \boldsymbol{v}_i, c_i^k)_{\Omega_i} + (\boldsymbol{D}_i^{-1} \boldsymbol{r}_i^k, \boldsymbol{v}_i)_{\Omega_i} & = \displaystyle\sum_{j \in \mathcal{N}_i} \int_{\Gamma_{i,j}} c_i^k (-\boldsymbol{v}_i \cdot \boldsymbol{n}_i), & \forall \boldsymbol{v}_i \in \tilde{\Sigma}_i. \end{array} \tag{4.15}$$

Choosing $\mu_i = c_i^k$ and $\boldsymbol{v}_i = \boldsymbol{r}_i^k$ in (4.15), then adding the two resulting equations and replacing the boundary term by using the equation

$$\begin{aligned} &\left(-\boldsymbol{r}_i^k \cdot \boldsymbol{n}_i + \alpha_{i,j} c_i^k\right)^2 - \left(-\boldsymbol{r}_i^k \cdot \boldsymbol{n}_i - \alpha_{j,i} c_i^k\right)^2 \\ &\qquad\qquad = 2\left(\alpha_{i,j} + \alpha_{j,i}\right) c_i^k \left(-\boldsymbol{r}_i^k \cdot \boldsymbol{n}_i\right) + \left(\alpha_{i,j}^2 - \alpha_{j,i}^2\right) \left(c_i^k\right)^2, \end{aligned}$$

we obtain

$$\begin{aligned} &\frac{1}{2} \frac{d}{dt}(\omega_i c_i^k, c_i^k)_{\Omega_i} + \left(\boldsymbol{D}_i^{-1} \boldsymbol{r}_i^k, \boldsymbol{r}_i^k\right)_{\Omega_i} + \sum_{j \in \mathcal{N}_i} \int_{\Gamma_{i,j}} \frac{1}{2\left(\alpha_{i,j} + \alpha_{j,i}\right)} \left(-\boldsymbol{r}_i^k \cdot \boldsymbol{n}_i - \alpha_{j,i} c_i^k\right)^2 \\ &= \sum_{j \in \mathcal{N}_i} \int_{\Gamma_{i,j}} \frac{1}{2\left(\alpha_{i,j} + \alpha_{j,i}\right)} \left(-\boldsymbol{r}_i^k \cdot \boldsymbol{n}_i + \alpha_{i,j} c_i^k\right)^2 + \frac{1}{2} \sum_{j \in \mathcal{N}_i} \int_{\Gamma_{i,j}} \left(\alpha_{j,i} - \alpha_{i,j}\right) \left(c_i^k\right)^2. \end{aligned}$$

We then integrate over $(0,t)$ for a.e. $t \in (0,T]$ and apply the Robin boundary conditions. By using the properties of ω and $\boldsymbol{D}$ and recalling that the Robin coefficients

$\alpha_{i,j}$ belong to $L^{\infty}\left(\Gamma_{i,j}\right)$, $i \in 1, \cdots, I$, $j \in \mathcal{N}_i$, we obtain, for some constant C,

$$\omega_{-}\|c_i^k\left(t\right)\|_{\Omega_i}^2 + 2\delta_{-}\int_0^t \|\boldsymbol{r}_i^k\left(s\right)\|^2 ds + \sum_{j\in\mathcal{N}_i}\int_0^t\int_{\Gamma_{i,j}} \frac{1}{\alpha_{i,j}+\alpha_{j,i}}\left(-\boldsymbol{r}_i^k\cdot\boldsymbol{n}_i - \alpha_{j,i}c_i^k\right)^2$$
$$\leq \sum_{j\in\mathcal{N}_i}\int_0^t\int_{\Gamma_{i,j}} \frac{1}{\alpha_{i,j}+\alpha_{j,i}}\left(-\boldsymbol{r}_j^{k-1}\cdot\boldsymbol{n}_i + \alpha_{i,j}c_j^{k-1}\right)^2 + C\int_0^t \|c_i^k\left(s\right)\|_{\Omega_i}^2 ds.$$

Now we sum over all subdomains and define for $k \geq 1$ and for a.e. $t \in (0, T]$

$$E^k\left(t\right) = \sum_{i=1}^{I}\left(\omega_{-}\|c_i^k\left(t\right)\|_{\Omega_i}^2 + 2\delta_{-}\int_0^t \|\boldsymbol{r}_i^k\left(s\right)\|^2 ds\right),$$
$$B^k\left(t\right) = \sum_{i=1}^{I}\sum_{j\in\mathcal{N}_i}\int_0^t\int_{\Gamma_{i,j}} \frac{1}{\alpha_{i,j}+\alpha_{j,i}}\left(-\boldsymbol{r}_j^k\cdot\boldsymbol{n}_i + \alpha_{i,j}c_j^k\right)^2.$$

Then we have, for all $k > 0$

$$E^k\left(t\right) + B^k\left(t\right) \leq B^{k-1}\left(t\right) + C\sum_{i=1}^{I}\int_0^t \|c_i^k\left(s\right)\|_{\Omega_i}^2 ds.$$

Now sum over the iterates for any given $K > 0$:

$$\sum_{k=1}^{K} E^k\left(t\right) \leq B^0\left(t\right) + C\sum_{k=1}^{K}\sum_{i=1}^{I}\int_0^t \|c_i^k\left(s\right)\|_{\Omega_i}^2 ds, \tag{4.16}$$

where

$$B^0\left(t\right) = \sum_{i=1}^{I}\sum_{j\in\mathcal{N}_i}\int_0^t\int_{\Gamma_{i,j}} \frac{1}{\alpha_{i,j}+\alpha_{j,i}}(g_{i,j})^2,$$

for $g_{i,j}$ the initial guess on $\Gamma_{i,j}$. From the definition of E^k, since $\delta_{-} > 0$, we have

$$\sum_{k=1}^{K}\sum_{i=1}^{I}\omega_{-}\|c_i^k\left(t\right)\|_{\Omega_i}^2 \leq B^0\left(t\right) + C\sum_{k=1}^{K}\sum_{i=1}^{I}\int_0^t \|c_i^k\left(s\right)\|_{\Omega_i}^2 ds.$$

Thus, by applying Gronwall's lemma, we obtain for any $K > 0$ and a.e. $t \in (0, T)$

$$\sum_{k=1}^{K}\sum_{i=1}^{I}\|c_i^k\left(t\right)\|_{\Omega_i}^2 \leq e^{\frac{CT}{\omega_{-}}}\frac{B^0\left(T\right)}{\omega_{-}}. \tag{4.17}$$

This along with (4.16) implies

$$\sum_{k=1}^{K}\sum_{i=1}^{I}2\delta_{-}\int_0^t \|\boldsymbol{r}_i^k\left(s\right)\|^2 ds \leq \left(1 + \frac{CT}{\omega_{-}}e^{\frac{CT}{\omega_{-}}}\right)B^0\left(T\right), \quad \forall K > 0. \tag{4.18}$$

The inequalities (4.17), (4.18) imply that the sequence c_i^k tends to 0 in $L^{\infty}\left(0, T; L^2\left(\Omega_i\right)\right)$ and $\boldsymbol{r}_i^k$ converges to 0 in $L^2\left(0, T; \boldsymbol{L^2(\Omega_i)}\right)$ for each $i \in 1, \cdots, I$ as $k \to \infty$.

To show convergence in higher norms, we differentiate the first and the second equations of (4.15) with respect to t, then take $\mu_i = \partial_t c_i^k$ and $\boldsymbol{v}_i = \partial_t \boldsymbol{r}_i^k$ and add the resulting equations together, we see that (after bounding the left hand side using the assumptions on ω and $\boldsymbol{D}$)

$$\frac{\omega_-}{2}\frac{d}{dt}\|\partial_t c_i^k\|_{\Omega_i}^2 + \delta_-\|\partial_t \boldsymbol{r}_i^k\|_{\Omega_i}^2 \le \sum_{j\in\mathcal{N}_i}\int_{\Gamma_{i,j}} \partial_t c_i^k(-\partial_t \boldsymbol{r}_i^k\cdot \boldsymbol{n}_i).$$

We proceed as in the previous argument with the use of Robin boundary conditions after differentiating with respect to t

$$-\partial_t \boldsymbol{r}_i^k\cdot\boldsymbol{n}_i + \alpha_{i,j}\partial_t c_i^k = -\partial_t \boldsymbol{r}_j^{k-1}\cdot\boldsymbol{n}_i + \alpha_{i,j}\partial_t c_j^{k-1}, \;\text{ on } \Gamma_{i,j}\times(0,T)\,, \forall j\in\mathcal{N}_i.$$

We then obtain, for all $k>0$

$$\tilde{E}^k(t) + \tilde{B}^k(t) \le \tilde{B}^{k-1}(t) + C\sum_{i=1}^{I}\int_0^t \|\partial_t c_i^k(s)\|_{\Omega_i}^2 ds.$$

where

$$\tilde{E}^k(t) = \sum_{i=1}^{I}\left(\omega_-\|\partial_t c_i^k(t)\|_{\Omega_i}^2 + 2\delta_-\int_0^t \|\partial_t \boldsymbol{r}_i^k(s)\|^2 ds\right),$$

$$\tilde{B}^k(t) = \sum_{i=1}^{I}\sum_{j\in\mathcal{N}_i}\int_0^t\int_{\Gamma_{i,j}} \frac{1}{\alpha_{i,j}+\alpha_{j,i}}\left(-\partial_t \boldsymbol{r}_j^k\cdot\boldsymbol{n}_i + \alpha_{i,j}\partial_t c_j^k\right)^2.$$

Now, as before, we sum over the iterates for any $K>0$ and apply Gronwall's lemma to obtain for any $K>0$ and a.e. $t\in(0,T)$

$$\sum_{k=1}^{K}\sum_{i=1}^{I}\|\partial_t c_i^k(t)\|_{\Omega_i}^2 \le e^{\frac{CT}{\omega_-}}\frac{\tilde{B}^0(T)}{\omega_-}, \quad \text{with } \tilde{B}^0(t) = \sum_{i=1}^{I}\sum_{j\in\mathcal{N}_i}\int_0^t\int_{\Gamma_{i,j}}\frac{1}{\alpha_{i,j}+\alpha_{j,i}}(\partial_t g_{i,j})^2. \tag{4.19}$$

This along with (4.17) shows that the sequence c_i^k converges to 0 in $W^{1,\infty}(0,T;L^2(\Omega_i)$ as $k\to\infty$, for $i = 1, \cdots, I$.
Now we choose $\mu_i = \nabla\cdot\boldsymbol{r}_i^k$ in the first equation of (4.15) to obtain for a.e. $t\in(0,T)$

$$\|\nabla\cdot\boldsymbol{r}_i^k\|^2 = -\left(\partial_t c_i^k, \nabla\cdot\boldsymbol{r}_i^k\right) \le \|\partial_t c_i^k\|\,\|\nabla\cdot\boldsymbol{r}_i^k\|.$$

or

$$\|\nabla\cdot\boldsymbol{r}_i^k\| \le \|\partial_t c_i^k\| \quad \forall t\in(0,T).$$

Hence, by (4.19) we have

$$\|\nabla\cdot\boldsymbol{r}_i^k\|_{L^\infty(0,T;L^2(\Omega_i))} \to 0 \text{ as } k\to\infty. \tag{4.20}$$

This shows that the sequence $\boldsymbol{r}_i^k$ converges to 0 in $L^2(0,T;H(\mathrm{div},\Omega_i))$. Moreover, it follows from the definition of $\tilde{E}^k$ and (4.19) that

$$\sum_{k=1}^{K}\sum_{i=1}^{I}2\delta_-\int_0^t\|\partial_t\boldsymbol{r}_i^k(s)\|^2 ds \le (1+\frac{CT}{\omega_-}e^{\frac{CT}{\omega_-}})\tilde{B}^0(T), \quad \forall K>0.$$

So that the sequence $\partial_t\boldsymbol{r}_i^k$ also converges to 0 in $L^2(0,T;\boldsymbol{L^2(\Omega_i)})$. $\square$

5. Nonconforming time discretizations and projections in time. One of the main advantages of Method 1 or Method 2 is that these methods are global in time and thus enable the use of independent time discretizations in the subdomains. At the space-time interface, data is transferred from one space-time subdomain to a neighboring subdomain by using a suitable projection.

We consider semi-discrete problems in time with nonconforming time grids. Let $\mathcal{T}_1$ and $\mathcal{T}_2$ be two possibly different partitions of the time interval $(0,T)$ into sub-intervals (see Figure 5.1). We denote by J_m^i the time interval $(t_{m-1}^i, t_m^i]$ and by $\Delta t_m^i := (t_m^i - t_{m-1}^i)$ for $m = 1, \dots, M_i$ and $i = 1, 2$, where for simplicity of exposition we have again supposed that we have only two subdomains. We use the lowest order discontinuous Galerkin method [3, 17, 33], which is a modified backward Euler method. The same idea can be generalized to higher order methods. We denote by $P_0(\mathcal{T}_i, W)$ the space of

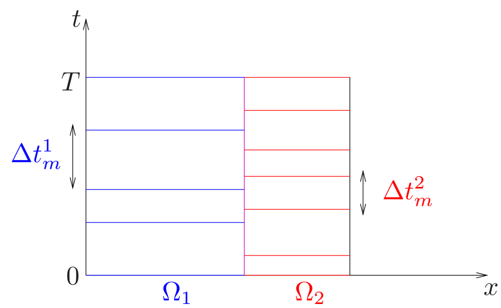

Figure 5.1: Nonconforming time grids in the subdomains.

piecewise constant functions in time on grid $\mathcal{T}_i$ with values in W, where $W = H^{\frac{1}{2}}(\Gamma)$ for Method 1 and $W = L^2(\Gamma)$ for Method 2:

$$P_0(\mathcal{T}_i, W) = \left\{ \phi : (0,T) \to W, \phi \text{ is constant on } J_m^i, \ \forall m = 1, \dots, M_i \right\}.$$

In order to exchange data on the space-time interface between different time grids, we define the following L^2 projection Π_{ji} from $P_0(\mathcal{T}_i, W)$ onto $P_0(\mathcal{T}_j, W)$ (see [12, 17]) : for $\phi \in P_0(\mathcal{T}_i, W)$, $\Pi_{ji}\phi|_{J_m^j}$ is the average value of ϕ on J_m^j, for $m = 1, \dots, M_j$:

$$\Pi_{ji}\left(\phi\right)|_{J_m^j} = \frac{1}{|\ J_m^j\ |} \sum_{l=1}^{M_i} \int_{J_m^j \cap J_l^i} \phi.$$

We use the algorithm described in [13] for effectively performing this projection. With these tools, we are now able to weakly enforce the transmission conditions over the time intervals.

We still denote by $(c_i, \boldsymbol{r}_i)$, for $i = 1, 2$, the solution of the problem semi-discrete in time corresponding to problem (4.7) or (4.12).

5.1. For Method 1. As there is only one unknown λ on the interface, we need to choose λ piecewise constant in time on one grid, either $\mathcal{T}_1$ or $\mathcal{T}_2$. For instance, let $\lambda \in P_0(\mathcal{T}_2, H^{\frac{1}{2}}(\Gamma))$ and take $c_2 = \Pi_{22}(\lambda) = \mathrm{Id}(\lambda)$. The weak continuity of the concentration in time across the interface is fulfilled by letting

$$c_1 = \Pi_{12}(\lambda) \in P_0(\mathcal{T}_1, H^{\frac{1}{2}}(\Gamma)).$$

The semi-discrete (nonconforming in time) counterpart of the flux continuity in the second equation of (4.2) is weakly enforced by integrating it over each time interval

J_m^2 of grid $\mathcal{T}_2$: $\forall m = 1, ..., M_2$,

$$\int_\Gamma \int_{J_m^2} \Big(\Pi_{21}\big(\boldsymbol{r}_1(\Pi_{12}(\lambda), f, c_0) \cdot \boldsymbol{n}_1\big) + \Pi_{22}\big(\boldsymbol{r}_2(\Pi_{22}(\lambda), f, c_0) \cdot \boldsymbol{n}_2\big) \Big)\, dt = 0. \tag{5.1}$$

Remark. Obviously one can choose λ to be constant in time on yet another grid (neither $\mathcal{T}_1$ nor $\mathcal{T}_2$), and this can be useful in some applications (e.g. flow in porous media with fractures).

5.2. For Method 2. In Method 2, there are two interface unknowns representing the Robin terms from each subdomain. Thus we let $\xi_i \in P_0(\mathcal{T}_i, L^2(\Gamma))$, for $i = 1, 2$. The semi-discrete in time counterpart of (4.3) is weakly enforced as follows:

$$\begin{aligned} &\int_\Gamma \int_{J_m^1} \Big(\xi_1 - \Pi_{12}\big(-\boldsymbol{r}_2(\xi_2, f, c_0) \cdot \boldsymbol{n}_1 + \alpha_{1,2} c_2(\xi_2, f, c_0)\big) \Big)\, dt = 0, \qquad \forall m = 1, \cdots, M_1, \\ &\int_\Gamma \int_{J_m^2} \Big(-\Pi_{21}\big(-\boldsymbol{r}_1(\xi_1, f, c_0) \cdot \boldsymbol{n}_2 + \alpha_{2,1} c_1(\xi_1, f, c_0)\big) + \xi_2 \Big)\, dt = 0, \quad \forall m = 1, \cdots, M_2, \end{aligned} \tag{5.2}$$

where $(c_i(\xi_i, f, c_0), \boldsymbol{r}_i(\xi_i, f, c_0))$, $i = 1, 2$ is the solution to (4.12).

Remark. For conforming time grids, the two schemes defined by applying GMRES for the two interface problems (5.1), (5.2) respectively converge to the same monodomain solution. In the nonconforming case, due to different projections, the two schemes become different and in the next section, we will study and compare the errors in time for the two approaches.

6. Numerical results. In this section, we carry out numerical experiments in 2D to illustrate the performance of the two methods presented above. We consider $\boldsymbol{D} = d\boldsymbol{I}$ isotropic and constant on each subdomain, where $\boldsymbol{I}$ is the 2D identity matrix. Consequently, we may denote by d_i, the diffusion coefficient in the subdomains. For the spatial discretization, we use mixed finite elements with the lowest order Raviart-Thomas spaces on rectangles [5, 30].

In the first test problem (see Section 6.1), we consider the two subdomain case with discontinuous coefficients. We vary the jumps in the diffusion coefficients and we see how it affects the convergence speed. We also analyze the behavior of the error versus the time steps in the nonconforming case. In the second test problem (see Section 6.2), suggested by ANDRA as a first step towards repository simulations, we consider several subdomains. We observe how both methods handle this application with the strong heterogeneity and long time computations.

6.1. A two subdomain case. The computational domain Ω is the unit square, and the final time is $T = 1$. We split Ω into two nonoverlapping subdomains $\Omega_1 = (0, 0.5) \times (0, 1)$ and $\Omega_2 = (0.5, 1) \times (0, 1)$ as depicted in Figure 6.1. The initial condition is $c_0 = \exp\big((x - 0.55)^2 + 0.5(y - 0.5)^2\big)$ and the right-hand side is $f = 0$. The porosity is $\omega_1 = \omega_2 = 1$, the diffusion coefficients are d_1 and d_2 in Ω_1 and Ω_2 respectively ($d_1 \neq d_2$). We fix $d_2 = 0.2$ and vary d_1 as shown in Table 6.1. We let $\mathfrak{D}$ denote the diffusion ratio d_2/d_1. For the spatial discretization, we use a uniform rectangular mesh with size $\Delta x_1 = \Delta x_2 = 1/200$. For the time discretization, we use nonconforming time grids with Δt_1 and Δt_2, given in Table 6.1, adapted to different diffusion ratios. We first analyze the convergence behavior of each method. We solve a problem with $c_0 = 0$ and $f = 0$ (thus $c = 0$ and $\boldsymbol{r} = 0$). We start with a random initial guess on the space-time interface. We remark that one iteration of Method 1

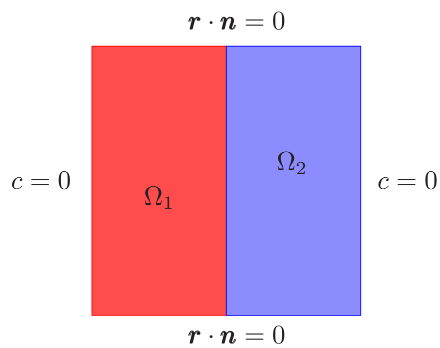

Figure 6.1: Domain decomposition and boundary conditions.

$\mathfrak{D}$	d_1	$1/\Delta t_1$	d_2	$1/\Delta t_2$
10	0.02	150	0.2	200
100	0.002	50	0.2	200
1000	0.0002	20	0.2	200

Table 6.1: Diffusion coefficients and corresponding nonconforming time steps.

with the preconditioner costs twice as much as one iteration of Method 2 (in terms of number of subdomain solves). Thus to compare the two approaches, we plot the error (in logarithmic scale) in the $L^2(0,T;L^2(\Omega))$-norm of the concentration c and the vector field $\boldsymbol{r}$, versus the number of subdomain solves (instead of versus the number of iterations). We stop the iteration when the errors (both in c and $\boldsymbol{r}$) are less than 10^{-6}. In Figure 6.2, the convergence of the two methods (with GMRES) for different diffusion ratios is shown. We see that both methods work well. Method 1 (Schur)

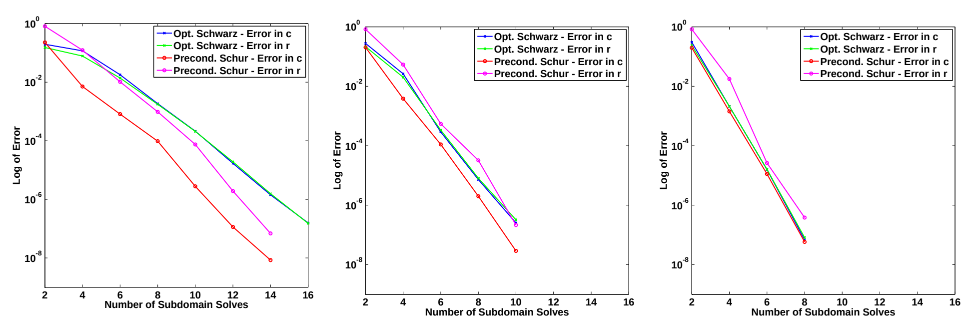

$\mathfrak{D} = 10$ $\mathfrak{D} = 100$ $\mathfrak{D} = 1000$

Figure 6.2: Convergence curves for different diffusion ratios: errors in c for Method 1 (red) and Method 2 (blue); errors in $\boldsymbol{r}$ for Method 1 (magenta) and Method 2 (green).

converges faster than Method 2 (Schwarz) for small diffusion ratios $\mathfrak{D}$. However, when $\mathfrak{D}$ is increased, they are comparable. We also observe that the errors in c and $\boldsymbol{r}$ are nearly the same for Method 2 while the error in $\boldsymbol{r}$ is greater than the error in c for Method 1. Both methods handle the heterogeneities efficiently. To obtain such a good performance, we have used the following formula for calculating the weights in (4.8) (see [25])

$$\sigma_i = \left(\frac{d_i}{d_1 + d_2}\right)^2, \quad i = 1, 2.$$

Consider now the case with $\mathfrak{D} = 10$. For Method 2, we vary Robin parameters $\alpha_{1,2}$ and $\alpha_{2,1}$ and plot the logarithmic scale of the residual after 20 Jacobi iterations in Figure 6.3. We see that the optimized Robin parameters (the red star), which are calculated by numerically minimizing the convergence factor [1, 2, 11], are located close to those giving the smallest residual after the same number of iterations.

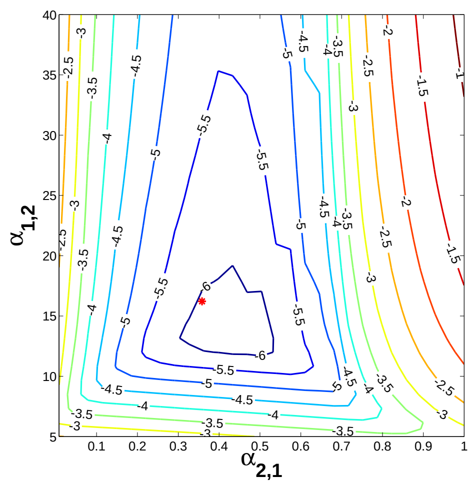

Figure 6.3: Level curves for the residual (in logarithmic scale) after 20 Jacobi iterations for various values of the parameters $\alpha_{1,2}$ and $\alpha_{2,1}$. The red star shows the optimized parameters computed by numerically minimizing the continuous convergence factor.

Next, we analyze the accuracy in time for different diffusion ratios and corresponding choices of nonconforming time steps. Toward this end, we consider four initial time grids (for Δt_c and Δt_f given)

- Time grid 1 (fine-fine): conforming with $\Delta t_1 = \Delta t_2 = \Delta t_f$.
- Time grid 2 (coarse-fine): nonconforming with $\Delta t_1 = \Delta t_c$ and $\Delta t_2 = \Delta t_f$.
- Time grid 3 (fine-coarse): nonconforming with $\Delta t_1 = \Delta t_f$ and $\Delta t_2 = \Delta t_c$.
- Time grid 4 (coarse-coarse): conforming with $\Delta t_1 = \Delta t_2 = \Delta t_c$.

The time steps are then refined several times by a factor of 2. In space, we fix a conforming rectangular mesh and we compute a reference solution by solving problem (2.4) directly on a very fine time grid, with $\Delta t = \Delta t_f / 2^6$. The converged multidomain solution is such that the relative residual is smaller than 10^{-11}. We show in Figures 6.4 and 6.5 the errors in the $L^2(0,T;L^2(\Omega))$-norms of the concentration c and the vector field $\boldsymbol{r}$ versus the time step $\Delta t = \max(\Delta t_c, \Delta t_f)$ for different diffusion ratios. We only give the results for Method 1 because the curves for Method 2 look exactly the same. For $\mathfrak{D} = 10$, we take $\Delta t_c = 1/94$ and $\Delta t_f = 1/128$; for $\mathfrak{D} = 100$, we take $\Delta t_c = 1/40$ and $\Delta t_f = 1/160$ (for $\mathfrak{D} = 1000$, the same results hold for $\Delta t_c = 1/16$ and $\Delta t_f = 1/160$ but we don't present it here). We first observe that first order convergence is preserved in the nonconforming case. Moreover, the error obtained in the nonconforming case (Time grid 2, in blue) is nearly the same as in the finer conforming case (Time grid 1, in red). This means that nonconforming time grids preserve the solution's accuracy in time and one must refine the time step where the solution varies most (i.e. where the diffusion coefficient is larger).

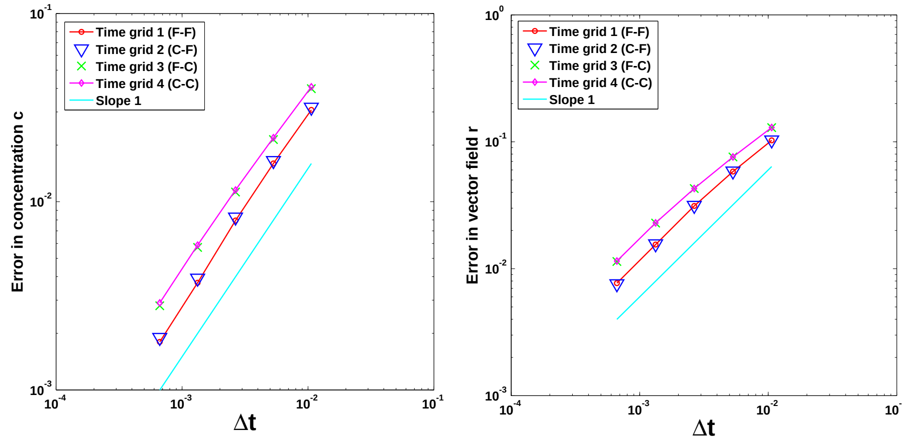

Figure 6.4: Errors in c (left) and $\boldsymbol{r}$ (right) in logarithmic scales between the reference and the multidomain solutions versus the time step for $\mathfrak{D} = 10$.

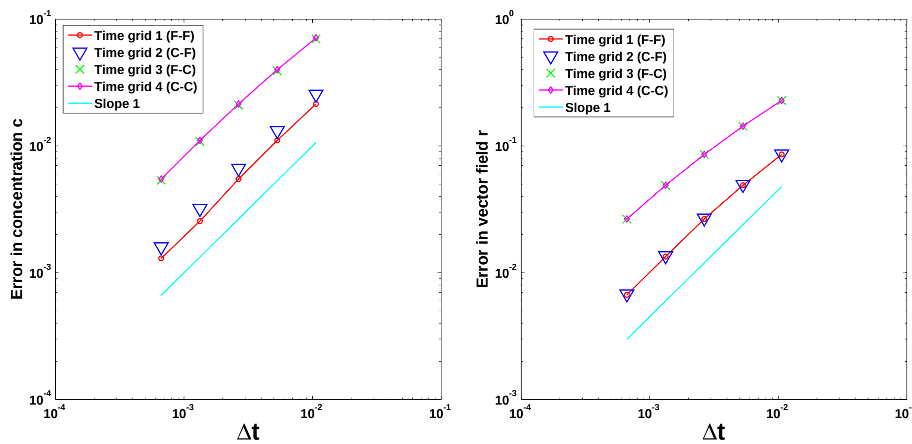

Figure 6.5: Errors in c (left) and $\boldsymbol{r}$ (right) in logarithmic scales between the reference and the multidomain solutions versus the time step for $\mathfrak{D} = 100$.

6.2. A porous medium test case. In this subsection, we consider a simplified version of a problem simulating contaminant transport in and around a nuclear waste repository site. The test case is described in Figure 6.6, where the repository is shown in red and the clay layer in yellow. The domain is a 3950m by 140m rectangle and the repository is a centrally located 2950m by 10m rectangle. The initial condition is $c_0 = 0$, the source term is $f = 0$ in the clay layer and

$$f = \begin{cases} 10^{-5}\ \mathrm{s}^{-1} & \text{if } t \leq 10^5 \text{ years}, \\ 0 & \text{if } t > 10^5 \text{ years}, \end{cases} \quad \text{in the repository.} \tag{6.1}$$

We impose homogeneous Dirichlet conditions on top and bottom, and homogeneous Neumann conditions on the left and right hand sides. We decompose Ω into 9 subdomains as depicted in Figure 6.7 with Ω_5 representing the repository. The porosity is $\omega_5 = 0.2$ and $\omega_i = 0.05$, $i \neq 5$. The diffusion coefficients are $d_5 = 2\,10^{-9}$ m^2/s and $d_i = 5\,10^{-12}$ m^2/s, $i \neq 5$. So the diffusion ratio is $\mathfrak{D} = 400$. For the spatial

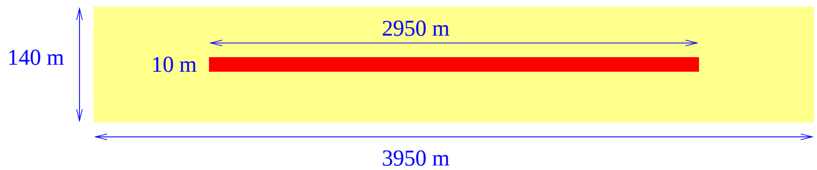

Figure 6.6: Geometry of the domain.

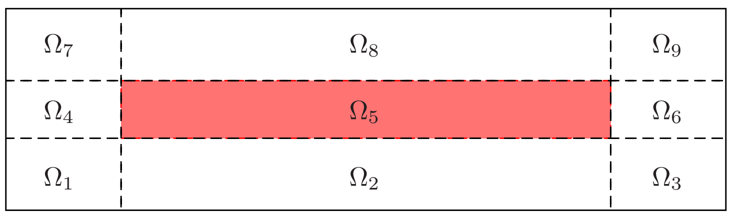

Figure 6.7: The decomposition into 9 subdomains (blow up in the y-direction).

discretization, we use a non-uniform but conforming rectangular mesh with a finer discretization in the repository (a uniform mesh with 600 points in the x direction and 30 points in the y direction) and a coarser discretization in the clay layer (the mesh size progressively increases with distance from the repository by a factor of 1.05). For the time discretization, we use nonconforming time grids with $\Delta t_5 = 2000$ years and $\Delta t_i = 10,000$ years, $i \neq 5$. For this application, we are interested in the long-term behaviour of the repository, say over one million years. Thus, we test the performance of the two methods for a "short" time interval ($T = 200,000$ years) and for a longer time interval ($T = 1,000,000$ years). The same time steps, Δt_i, are used for both cases. As in the first test problem, we analyze the convergence results by solving a problem with $f = 0$. For Method 2, as we have a small, thin object embedded in a large area, it has been shown in [16, 20] that it is important to derive an adapted optimization for Robin parameters. Thus, we consider two different optimization techniques: the classical one (Opt. 1) as used in the first test problem, and an adapted version (Opt. 2) [16, 20] where we take into account the dimension of the subdomains.

In Figure 6.8 we compare the errors in the concentration c (on the left) and in the vector field $\boldsymbol{r}$ (on the right) both over a shorter time interval (on top) and over a longer time interval (on bottom) where GMRES is used in all cases as the iterative solver: Method 1 (red), Method 2 with Opt. 1 (blue) and Method 2 with Opt. 2 (green). They are comparable and perform well in the case of multiple subdomains. We also note that the longer the time interval, the larger the number of subdomain solves needed to converge to a given tolerance (here 10^{-6}). Thus, the use of time windows (see [3, 18]) could considerably improve the performance of all the algorithms, especially with an adapted choice of the initial guess on the interface based on the solution on the previous time window. In Figure 6.9, we plot the errors in the concentration c over different time intervals for Method 2 with Jacobi iteration: with Opt. 1 (blue) and Opt. 2 (green) (the errors in the vector field $\boldsymbol{r}$ behave similarly). We observe that Opt. 2 efficiently handles the long time computation case while Opt. 1 doesn't.

Next we consider the case with $f \neq 0$ as defined in (6.1) and over the long time interval, $T = 1,000,000$ years. The discretizations in space and in time (nonconform-

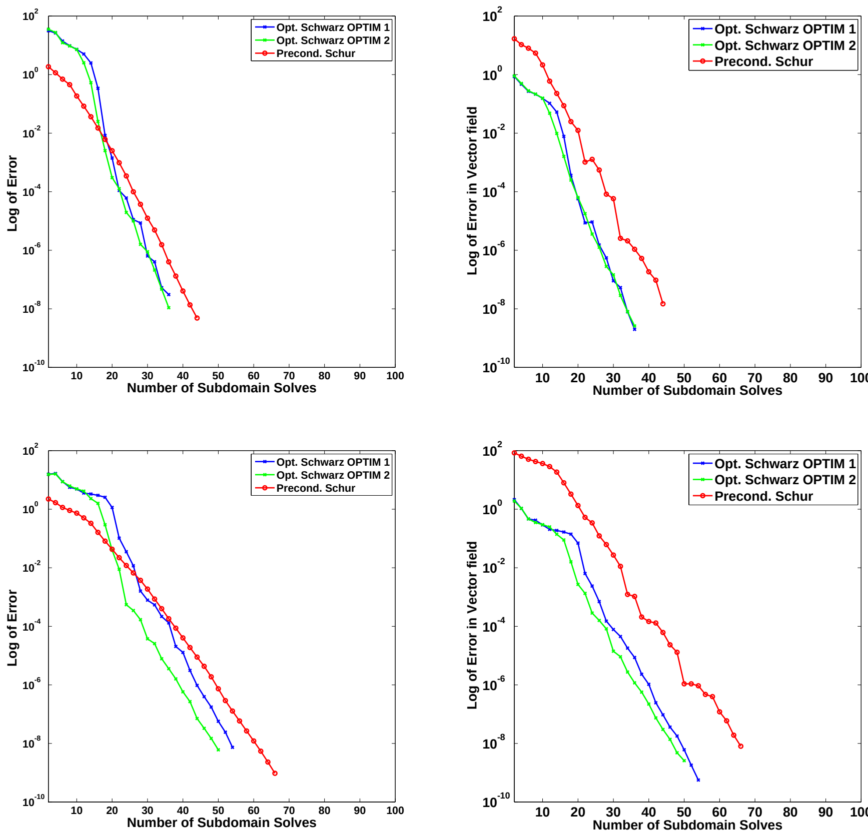

Figure 6.8: Convergence curves for different time intervals with GMRES: error in c (on the left) and error in $\boldsymbol{r}$ (on the right), for short time $T = 200,000$ years (on top) and for long time $T = 1,000,000$ years (on bottom).

ing) are the same as above. We verify the performance of Method 1 and Method 2 (with Opt. 2) using GMRES and zero initial guess on the space-time interfaces. The tolerance of the iteration is 10^{-6}. In Figure 6.10, the evolution of the solution at different times is depicted (both methods give similar results). As time goes on and under the effect of diffusion, the contaminant slowly migrates from the repository to the surrounding area. Moreover, its concentration c increases until injection stops (i.e. after 100,000 years) and then decreases. In Figure 6.11 the relative residuals for each method versus the number of subdomain solves are shown, as the monodomain solution with nonconforming grids is unknown. Both methods work well and we observe that Method 1 converges linearly while Method 2 initially converges extremely rapidly, the convergence becoming linear after the first few iterations.

7. Conclusion. We have given mixed formulations for two different interface problems for the diffusion equation, one using the time-dependent Steklov-Poincaré operator and the other using OSWR with Robin transmission conditions on the space-time interfaces between subdomains. The subdomain problem with Robin boundary conditions is proved to be well-posed. A convergence proof of the OSWR algorithm in mixed form is also given. Nonconforming time grids are considered and a suitable

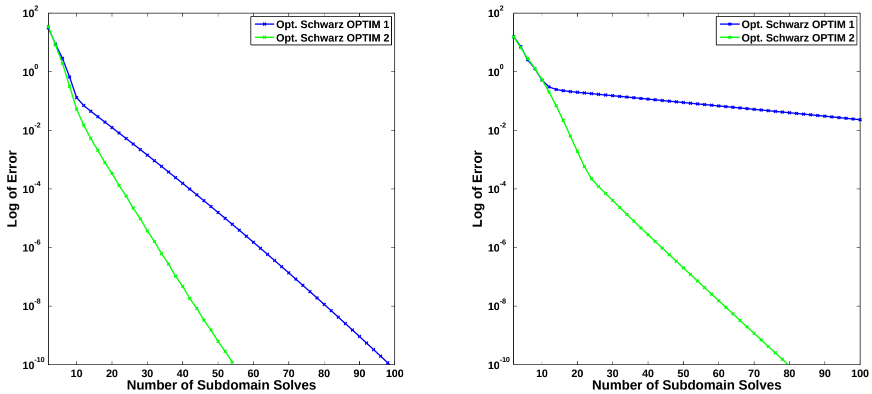

Figure 6.9: Convergence curves for different time intervals using Jacobi iteration: for short time $T = 200,000$ years (on the left) and for long time $T = 1,000,000$ years (on the right).

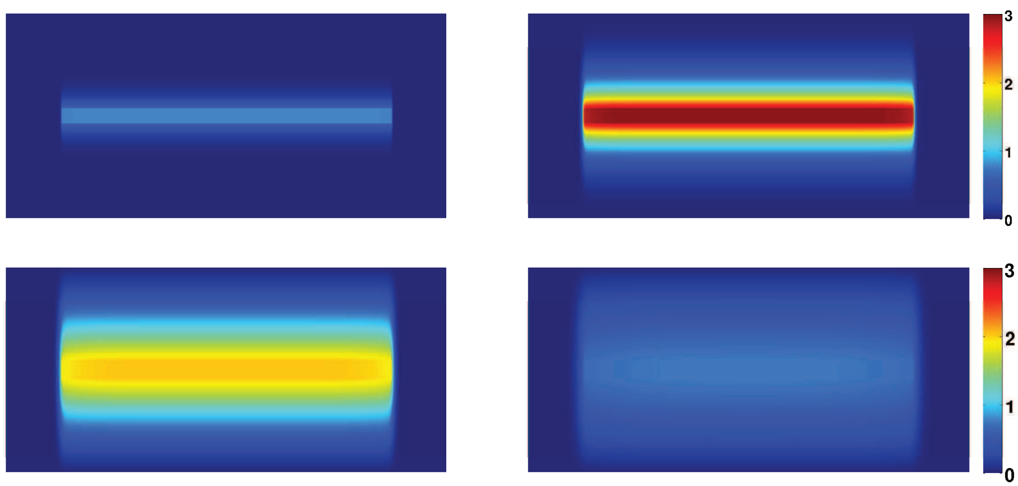

Figure 6.10: Snapshots of the multi-domain solution after 20,000 years (top left), 100 000 years (top right), 200 000 years (bottom left), and 1,000,000 years (bottom right), with a blow up in the y-direction.

projection in time is employed to exchange information between subdomains on the space-time interface. Numerical results for 2D problems using mixed finite elements (with the lowest order Raviart-Thomas spaces on rectangles) for discretization in space and the lowest order discontinuous Galerkin method for discretization in time are presented. We have analyzed numerically the performance of the two methods for two test cases, one academic with two subdomains and one more realistic with several subdomains. We have observed that both methods handle well the heterogeneity and nonconforming time grids, both efficiently preserving the solution's accuracy in time. The two methods are also well-adapted for the simulation of diffusive contaminant transport in and around a repository with a special geometry and long time computations. In particular, for Method 2 we have shown that an adapted optimization technique to compute the optimized parameters is necessary if Jacobi iteration is used. We have pointed out the possible advantage for efficiency of using time windows

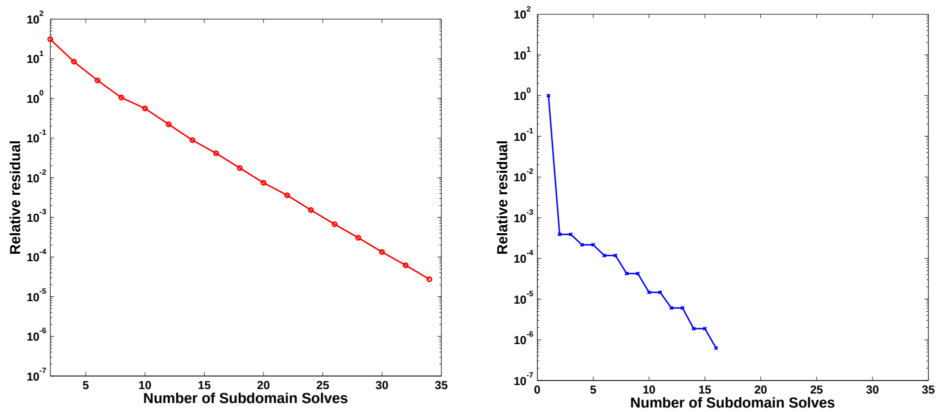

Figure 6.11: The relative residuals in logarithmic scales using GMRES for Method 1 (on the left) and Method 2 (with Opt. 2) (on the right).

for problems with long time interval. Work underway addresses the coupling between advection and diffusion using operator splitting as well as nonmatching grids in space.

REFERENCES

[1] D. Bennequin, M. J. Gander, and L. Halpern, *A homographic best approximation problem with application to optimized Schwarz waveform relaxation*, Math. Comp., 78 (2009), pp. 185–223.

[2] E. Blayo, L. Debreu, and F. Lemarié, *Toward an optimized global-in-time Schwarz algorithm for diffusion equations with discontinuous and spatially variable coefficients. Part 1: the constant coefficients case*, Accepted in ETNA.

[3] E. Blayo, L. Halpern, and C. Japhet, *Optimized Schwarz waveform relaxation algorithms with nonconforming time discretization for coupling convection-diffusion problems with discontinuous coefficients*, in Domain decomposition methods in science and engineering XVI, vol. 55 of Lect. Notes Comput. Sci. Eng., Springer, Berlin, 2007, pp. 267–274.

[4] D. Boffi and L. Gastaldi, *Analysis of finite element approximation of evolution problems in mixed form*, SIAM J. Numer. Anal., 42 (2004), pp. 1502–1526.

[5] F. Brezzi and M. Fortin, *Mixed and hybrid finite elements methods*, Springer-Verlag, New York, 1991.

[6] L. C. Cowsar, J. Mandel, and M. F. Wheeler, *Balancing domain decomposition for mixed finite elements*, Math. Comp., 64 (1995), pp. 989–1015.

[7] J. Douglas, Jr., P. J. Paes-Leme, J. E. Roberts, and J. P. Wang, *A parallel iterative procedure applicable to the approximate solution of second order partial differential equations by mixed finite element methods*, Numer. Math., 65 (1993), pp. 95–108.

[8] L. C. Evans, *Partial differential equations*, American Mathematical Society, Providence, 1998.

[9] L. Gander, M. J. Halpern and F. Nataf, *Optimal convergence for overlapping and non-overlapping Schwarz waveform relaxation*, in 11th International Conference on Domain Decomposition Methods, C-H. Lai, P. Bjørstad, M. Cross, and O. Widlund, eds., 1999, pp. 27–36.

[10] M. J. Gander and L. Halpern, *Optimized Schwarz waveform relaxation methods for advection reaction diffusion problems*, SIAM J. Numer. Anal., 45 (2007), pp. 666–697.

[11] M. J. Gander, L. Halpern, and M. Kern, *A Schwarz waveform relaxation method for advection-diffusion-reaction problems with discontinuous coefficients and non-matching grids*, in Domain decomposition methods in science and engineering XVI, vol. 55 of Lect. Notes Comput. Sci. Eng., Springer, Berlin, 2007, pp. 283–290.

[12] M. J. Gander, L. Halpern, and F. Nataf, *Optimal Schwarz waveform relaxation for the one dimensional wave equation*, SIAM J. Numer. Anal., 41 (2003), pp. 1643–1681.

[13] M. J. Gander, C. Japhet, Y. Maday, and F. Nataf, *A new cement to glue nonconforming grids with Robin interface conditions: the finite element case*, in Domain decomposition methods in science and engineering, vol. 40 of Lect. Notes Comput. Sci. Eng., Springer,

Berlin, 2005, pp. 259–266.

[14] F. Haeberlein, *Time space domain decomposition methods for reactive transport - Application to CO_2 geological storage*, PhD thesis, Institut Galilée, Université Paris 13, 2011.

[15] L. Halpern and C. Japhet, *Discontinuous Galerkin and Nonconforming in Time Optimized Schwarz Waveform Relaxation for Heterogeneous Problems*, in Decomposition Methods in Science and Engineering XVII, U. Langer, M. Discacciati, D.E. Keyes, O.B. Widlund, and W. Zulehner, eds., vol. 60 of Lecture Notes in Computational Science and Engineering, Springer, 2008, pp. 211–219.

[16] L. Halpern, C. Japhet, and P. Omnes, *Nonconforming in time domain decomposition method for porous media applications.*, in Proceedings of the 5th European Conference on Computational Fluid Dynamics ECCOMAS CFD 2010., J. C. F. Pereira and A. Sequeira, eds., Lisbon, Portugal, 2010.

[17] L. Halpern, C. Japhet, and J. Szeftel, *Discontinuous Galerkin and nonconforming in time optimized Schwarz waveform relaxation*, in Domain decomposition methods in science and engineering XIX, vol. 78 of Lect. Notes Comput. Sci. Eng., Springer, Heidelberg, 2011, pp. 133–140.

[18] ———, *Optimized Schwarz waveform relaxation and discontinuous Galerkin time stepping for heterogeneous problems*, SIAM J. Numer. Anal., 50 (2012), pp. 2588–2611.

[19] T. T. P. Hoang, J. Jaffré, C. Japhet, M. Kern, and J. E. Roberts, *Space-time domain decomposition for mixed formulations of diffusion equations.*, in Proceedings of the 21st International Conference on Domain Decomposition Methods., (to appear).

[20] C. Japhet and P. Omnes, *Optimized Schwarz waveform relaxation for porous media applications.*, in Proceedings of the 20th International Conference on Domain Decomposition Methods., 2013.

[21] F. Kwok, *Neumann-Neumann waveform relaxation for the time-dependent heat equation.*, in Proceedings of the 21st International Conference on Domain Decomposition Methods., (to appear).

[22] P. Le Tallec, Y. H. De Roeck, and M. Vidrascu, *Domain decomposition methods for large linearly elliptic three-dimensional problems*, J. Comput. Appl. Math., 34 (1991), pp. 93–117.

[23] J. Li, T. Arbogast, and Y. Huang, *Mixed methods using standard conforming finite elements*, Comput. Methods Appl. Mech. Engrg., 198 (2009), pp. 680–692.

[24] J. Mandel, *Balancing domain decomposition*, Comm. Numer. Methods Engrg., 9 (1993), pp. 233–241.

[25] J. Mandel and M. Brezina, *Balancing domain decomposition for problems with large jumps in coefficients*, Math. Comp., 65 (1996), pp. 1387–1401.

[26] V. Martin, *An optimized Schwarz waveform relaxation method for the unsteady convection diffusion equation in two dimensions*, Appl. Numer. Math., 52 (2005), pp. 401–428.

[27] W. Martinson and P. Barton, *A differentiation index for partial differential-algebraic equations*, SIAM Journal on Scientific Computing, 21 (2000), pp. 2295–2315.

[28] T. Mathew, *Domain Decomposition Methods for the Numerical Solution of Partial Differential Equations*, vol. 61 of Lecture Notes in Computational Science and Engineering, Springer, 2008.

[29] A. Quarteroni and A. Valli, *Domain decomposition methods for partial differential equations*, Clarendon Press, Oxford New York, 1999.

[30] J. E. Roberts and J.-M. Thomas, *Mixed and hybrid methods*, in Handbook of numerical analysis, Vol. II, Handb. Numer. Anal., II, North-Holland, Amsterdam, 1991, pp. 523–639.

[31] R. E. Showalter, *Nonlinear degenerate evolution equations in mixed formulation*, SIAM J. Math. Anal., 42 (2010), pp. 2114–2131.

[32] U. Stefanelli and A. Visintin, *Some nonlinear evolution problems in mixed form*, Boll. Unione Mat. Ital. (9), 2 (2009), pp. 303–320.

[33] V. Thomée, *Galerkin finite element methods for parabolic problems*, Springer, Berlin New York, 1997.

[34] A. Toselli and O. Widlund, *Domain decomposition methods—algorithms and theory*, vol. 34 of Springer Series in Computational Mathematics, Springer-Verlag, 2005.

RESEARCH CENTRE
PARIS – ROCQUENCOURT

Domaine de Voluceau, - Rocquencourt
B.P. 105 - 78153 Le Chesnay Cedex

Publisher
Inria
Domaine de Voluceau - Rocquencourt
BP 105 - 78153 Le Chesnay Cedex
inria.fr

ISSN 0249-6399